

## Supplemental Materials and Methods

**Reagents and antibodies.** ARV-825, ARV-771, ARV-766 and OTX015 were kindly provided by Arvinas, Inc. JQ1, R-JQ1, cytarabine and ABT-199 were obtained from Selleck Chemicals (Houston, TX). CD1530, Mevastatin, decitabine and doxycycline were obtained from Sigma-Aldrich (St. Louis, MO). Cinobufagin, anisomycin, narciclasine and fenbendazole were obtained from MedChem Express (Monmouth Junction, NJ). AI-4-88 and AI-10-104 were synthesized in the laboratory of John H. Bushweller (University of Virginia, Charlottesville, VA). All compounds were prepared as 10 mM stocks in 100% DMSO and frozen at -80°C in 5-10 µL aliquots (AI-4-88 and AI-10-104 were stored at room temperature) to allow for single use, thus avoiding multiple freeze-thaw cycles that could result in compound decomposition and loss of activity. Anti-BRD4 A301-985A100 (RRID: AB\_2620184) and anti-BRD2 A302-582A (RRID:AB\_2034828) antibodies were obtained from Bethyl Labs (Montgomery, TX). Anti-AML1 (RUNX1) [RRID:AB\_2184097], anti-c-Myc [RRID:AB\_1903938], anti-c-Myb [RRID:AB\_2716637], anti-PU.1 [RRID:AB\_10693421], anti-HEXIM1 [Cat #12604], anti-p21 [RRID:AB\_823586], anti-p-Histone H2AX (Ser139) [RRID:AB\_2118010] and anti-Bcl-xL [RRID:AB\_10695729] antibodies were obtained from Cell Signaling Technologies (Beverly, MA). Anti-CDK4 [RRID:AB\_631221], anti-CDK6 [RRID:AB\_10610066], anti-Bcl2 [RRID:AB\_626733], and anti-β-Actin [RRID:AB\_626630] antibodies were obtained from Santa Cruz Biotechnologies (Santa Cruz, CA). Anti-H3K27Ac Clone: MABI 0309 [RRID:AB\_11126964] antibody for ChIP was obtained from Active Motif (Carlsbad, CA). Rabbit monoclonal BRD4 antibody (chIP grade) A700-004 (RRID:AB\_2631885), rabbit polyclonal EP300 antibody A300-358A (RRID:AB\_185565)

**Oligonucleotide primers-** The sequences of primers utilized in these studies are provided in Supplemental Table S4.

**Cell lines and cell culture.** Human AML cell lines Mono-Mac-1 [ACC-252; RRID:CVCL\_1425], OCI-AML5 [ACC-247;RRID:CVCL\_1620], MOLM13 [DSMZ Cat# ACC-554, RRID:CVCL\_2119] and OCI-AML2 [ACC-99; RRID:CVCL\_1619] cells were obtained from the DSMZ. HEL92.1.7 [TIB-180; RRID:CVCL\_2481], MV4-11 [ATCC Cat# CRL-9591, RRID:CVCL\_0064] and THP1 [TIB-202; RRID:CVCL\_0006] cells were obtained from the ATCC (Manassas, VA). All experiments with cell lines were performed within 6 months after thawing or obtaining from ATCC or DSMZ. The cell lines were also authenticated in the Characterized Cell Line Core Facility at M.D. Anderson Cancer Center, Houston TX. Mono-Mac-1, HEL92.1.7, MOLM13 and THP1 cells were cultured in RPMI media with 20% FBS and 1% penicillin/streptomycin. MV4-11 cells were cultured in IMDM media with

20% FBS and 1% penicillin/streptomycin. OCI-AML5 and OCI-AML2 cells were cultured in MEM alpha media with 20% FBS and 1% penicillin/streptomycin. OCI-AML5 cultures were also supplemented with 10 ng/mL of GM-CSF (PeproTech, Rocky Hill, NJ). Logarithmically growing cells were utilized for all experiments. Following drug treatments, cells were washed free of the drug(s) prior to the performance of the studies described.

**Primary AML blast cells.** Patient-derived (PD) mutant RUNX1 and wild-type RUNX1 expressing AML cells and normal cord blood samples were obtained with informed consent as part of a clinical protocol approved by the Institutional Review Board of The University of Texas, M.D. Anderson Cancer Center. Mononuclear cells were purified by Ficoll Hypaque density centrifugation. Mononuclear cells were washed with complete RPMI media containing 20% FBS. CD34+ AML blast progenitor cells and banked, de-linked and de-identified, normal cord blood CD34+ cells were purified by immunomagnetic beads conjugated with anti-CD34 antibody (StemCell Technologies, Vancouver, British Columbia) and re-suspended in 20% FBS containing RPMI-1640 media prior to utilization in the cell viability assays and immunoblot analyses.

**Sequencing of primary AML cells.** We performed targeted next-generation sequencing (NGS) of DNA samples from bone marrow or peripheral blood collected from patients at our center with AML as described<sup>1</sup>. Diagnostic bone marrow samples were obtained for mutational analysis. Total genomic DNA was extracted from unenriched peripheral blood (PB) or bone marrow (BM) samples using ReliaPrep genomic DNA isolation kit (Promega Corp, Madison, WI, USA). FLT3 (internal tandem duplication and D835) was assessed by PCR followed by capillary electrophoresis on a Genetic Analyzer (Applied Biosystems, Foster City, CA, USA). Briefly, a total of 250 ng DNA was utilized to prepare sequencing libraries using Agilent HaloPlex custom Kit (Agilent Technologies, Santa Clara, CA, USA). The entire coding sequences of 28 genes (ABL1, ASXL1, BRAF, DNMT3A, EZH2, FLT3, GATA1, GATA2, HRAS, IDH1, IDH2, IKZF2, JAK2, KIT, KRAS, MDM2, MLL, MPL, NPM1, NRAS, PTPN11, RUNX1, TET2, TP53, WT1) were interrogated on a custom-designed next-generation sequencing approach using the Illumina MiSeq platform (Illumina; San Diego, CA, USA). The genomic reference sequence used was genome GRCh37/hg19. The following software tools were utilized in the experimental setup and data analysis: Illumina Experiment Manager 1.6.0 (Illumina; San Diego, CA, USA), MiSeq Control Software 2.4 (Illumina; San Diego, CA, USA), Real Time Analysis 1.18.54 (Illumina; San Diego, CA, USA), Sequence Analysis Viewer 1.8.37 (Illumina; San Diego, CA, USA), MiSeq Reporter 2.5.1 (Illumina; San Diego, CA, USA), and SureCall 3.0.1.4 (Agilent Technologies;

Santa Clara, CA, USA). A minimum of 80% reads at quality scores of AQ30 or higher were required to pass quality control. NM\_001754 was utilized as the RUNX1 reference sequence. The lower limit of detection of this assay (analytical sensitivity) for single nucleotide variations was determined to be 5% (one mutant allele in the background of nineteen wild type alleles) to 10% (one mutant allele in the background of nine wild type alleles). Testing of patients with active hematologic malignancies was limited to somatic mutations only.

**Plasmid Generation, Viral Packaging, and Creation of Cell Lines.** Five Runx1 shRNA (SHCLNG-NM\_001754) validated for the greatest knockdown of Runx1 were purchased from Sigma-Aldrich (St. Louis, MO). pLKO.1 Runx1 shRNA was transfected utilizing PEI (Polyethylenimine; PolySciences, Warrington, PA) with packaging plasmids psPAX2 and pMD2.G into HEK293T [RRID: CVCL\_0063]. The psPAX2 and pMD2.G packaging plasmids were a gift from Didier Trono (Addgene plasmid # 12260 and 12259). A 3:1 ratio of DNA to PEI (1  $\mu\text{g}/\mu\text{L}$ ) was employed in the transfection. Media was changed the following day. Viral supernatant was collected 72 hours post transfection, filtered through a 0.45  $\mu\text{m}$  PES membrane and used immediately or stored at 4°C for up to 2 weeks. OCI-AML5 cells were seeded at  $5 \times 10^5$  cells/mL in a 50:50 mix of media and lentiviral supernatant along with 8  $\mu\text{g}/\text{mL}$  of polybrene. The next day, the viral supernatant was removed by centrifugation and cells were transduced a second time with fresh viral supernatant. Seventy two hours after the first transduction, cells were harvested and cell lysates were analyzed for Runx1 knockdown by immunoblot analysis. For BRD4 knockdown, 5 shRNAs were obtained from Sigma-Aldrich (SHCLNG-NM\_058243) and validated for the greatest knockdown of BRD4 in the AML cell lines.

The Runx1 shRNA (TRCN0000338490), identified to display the most robust knockdown, was subcloned into Tet-pLKO-puro<sup>2</sup>. Tet-pLKO-puro was a gift from Dmitri Wiederschain (Addgene plasmid # 21915). The Runx1 shRNA oligonucleotides designed by the Broad Institute (Cambridge, MA) were purchased from Sigma. The ssDNA oligonucleotides were annealed to each other (5  $\mu\text{L}$  of each 100  $\mu\text{M}$  stock) in 40  $\mu\text{L}$  of annealing buffer (10 mM Tris pH 8.0, 50 mM NaCl, 1 mM EDTA pH 8.0) utilizing a thermocycler set to incrementally decrease the temperature from 95°C to 10°C (-0.6°C every 150 sec). The Runx1 shRNA annealed oligo insert was then ligated into *AgeI/EcoRI* digested Tet-pLKO-puro utilizing T4 DNA ligase and incubating in a thermocycler at 16°C overnight. Tetracycline-inducible Runx1 shRNA virus was produced as described above and transduced into OCI-AML5 cells. OCI-AML5 cells were then selected with 0.5  $\mu\text{g}/\text{mL}$  puromycin for one week. Luciferase-expressing OCI-

AML5 cells were created by transducing cells with Luc-ZsGreen containing lentiviral particles. pHIV-Luc-ZsGreen was a gift from Bryan Welm (Addgene plasmid # 39196).

**Colony growth and cell proliferation.** After the designated treatments, cells were harvested and washed twice with 1× PBS. Serial dilutions of the cells were prepared and approximately 500 cells were plated in complete Methocult (StemCell Technologies, Cambridge, MA) and cultured for 7 to 10 days at 37°C in a 5% CO<sub>2</sub> environment. Colonies were counted with an inverted light microscope at 4X magnification. Colony growth of treated cells was measured as a percentage of the control cell colony growth. For cell proliferation analysis, cells were plated in triplicate at 0.125 million cells/mL and cell numbers were counted utilizing a Countess-2 cell counting instrument (Life Technologies, Carlsbad, CA) every 24 hours for 72-96 hours.

**RNA isolation and quantitative polymerase chain reaction.** Following the designated treatments with ARV-825, ARV-771, or OTX015, total RNA was isolated from AML cells utilizing a PureLink RNA Mini kit from Ambion, Inc. (Austin, TX) and reverse transcribed. Quantitative real time PCR analysis for the expression of MYC, BCL-2, BCL2L1 (Bcl-xL), RUNX1, HEXIM1 and CDKN1A (p21) was performed on cDNA using TaqMan probes from Applied Biosystems (Foster City, CA). Relative mRNA expression was normalized to the expression of GAPDH and compared to the untreated cells.

**Analysis of epigenetic state in AML cells *in vitro*.** We used publicly available ChIP-Seq data of BRD4 from MOLM14 cells (GSE65161)<sup>3</sup>. Sequenced reads were mapped to the human genome UCSC build hg19/NCBI build 37 using BWA<sup>4</sup>. High-resolution genome-wide maps were derived and visualized in the UCSC Genome Browser (<http://genome.ucsc.edu/>) and using IGV software<sup>5,6</sup>. We also performed ATAC-Seq analysis of OCI-AML5 cells following a previously described protocol<sup>7</sup>. ATAC libraries were amplified for 10-12 cycles by PCR<sup>7</sup>. The amplified libraries were cleaned over a Qiagen MinElute column and eluted in 25 µL of 10 mM Tris, (pH 8.5). Excess Illumina adapters were removed utilizing a 1X bead concentration of AmpPure-XP beads and the library DNA was eluted in 20 µL of 10 mM Tris, (pH 8.5). The individual libraries were quantified and quality-checked by Qubit fluorometric quantification and with an Agilent 2100 Bioanalyzer. Individual libraries were pooled into one tube and sequenced on a NextSeq 500 next generation sequencer utilizing a 150-cycle mid-output kit (Illumina, San Diego, CA). Sequence tracks were visualized with IGV software as above<sup>5,6</sup>. We also determined the H3K27Ac status in OCI-AML5 by ChIPmentation following a previously described protocol<sup>8</sup>, with modifications on the concentration of AmpPure-XP beads utilized for dual SPRI selection. We utilized 0.65X beads for the first selection, then a 1.0X bead concentration to narrow the fragment size of the

final tagmented ChIP DNA library. The individual libraries were quantified and quality checked by Qubit and Agilent 2100 Bioanalyzer analysis as above. The libraries were pooled into one tube at equal concentrations of library DNA, purified over a Qiagen MinElute column, and eluted in 20  $\mu$ L. The pooled libraries were sequenced on a NextSeq 500 sequencer utilizing a 150-cycle mid output kit (Illumina, San Diego, CA). Sequence tracks were visualized with IGV software<sup>5, 6</sup>. To identify super enhancers within the ChIP DNA of OCI-AML5 and in the publicly available MOLM14 H3K27Ac ChIP Seq dataset<sup>3</sup>, we performed a rank order of super enhancers (ROSE) analysis utilizing the H3K27Ac status of the chromatin according to a previously described method utilizing default settings<sup>9</sup>.

**Hi-C analysis of RUNX1 intragenic interactions.** We used publicly available Hi-C data from K562 cells as part of the ENCODE project to visualize the promoter and enhancer interactions within the RUNX1 gene<sup>10</sup>. High-scoring interactions between the promoter and enhancer regions of RUNX1 are deeper red than lower scoring interactions.

**Chromatin immunoprecipitation and Real Time Polymerase Chain Reaction.** OCI-AML5 cells were treated with concentrations of OTX015 or ARV-771 for 8-16 hours. Following drug exposure, cross-linking, cell lysis, sonication and chromatin immunoprecipitation for BRD4 was performed according to the manufacturer's protocol (Millipore). For quantitative assessment of binding of BRD4, EP300, c-Myc, PU.1 and pSer2-RNAP2 to the RUNX1 +24 kb enhancer in the chromatin immunoprecipitates, a SYBR Green PCR Mastermix from Applied Biosystems was used (Foster City, CA). Relative enrichment of the DNA in the chromatin immunoprecipitates was normalized against the amount of RUNX1 +24 kb enhancer DNA in the input samples.

**Transcriptome Analysis.** Following the designated treatments with ARV-825 or OTX015 for 4 hours, RNA was isolated from cultured AML cells as biologic triplicates and sequencing libraries were prepared in the MD Anderson Cancer Center DNA Sequencing and Microarray core facility and sequenced on an Illumina HiSeq 4000 next generation sequencer. Each library yielded 30-40 million read pairs. Data was mapped using TopHat2 [RRID:SCR\_013035]<sup>11,12</sup> onto the human genome build UCSC hg19/(NCBI-37). Gene expression was assessed using Cufflinks2 [RRID:SCR\_014597]<sup>12</sup>, then variance stabilization and quantile normalization were applied. Significantly altered transcripts were determined using the limma package<sup>13</sup> in R; multiple hypotheses testing correction was applied using the false discovery rate (fdr) method implemented in the R statistical system. We considered that significance was achieved for fold changes greater than or equal to 1.5X or less than or equal to 0.5x

relative to the untreated cells, and p-values less than 0.05. Datasets have been deposited in GEO under Accession number (GSE119261).

**LINCS analysis-** A ranked list of chemical compounds associated with the RUNX1 shRNA signature was generated using the Library of Integrated Cellular Signatures (LINCS)/Connectivity Map compendia [RRID:SCR\_002639]<sup>14, 15</sup>. Specifically, significant gene alterations were first separated into up-regulated and down-regulated gene sets, and LINCS was involved programmatically via their API. A ranked summary of the chemical compounds, over-expression of selected proteins, and suppression of selected genes, was generated, and ranked by association with the RUNX1 shRNA signatures in OCI-AML5 cells.

**Assessment of apoptosis by annexin-V staining.** Untreated or drug-treated cells were stained with Annexin-V (Pharmingen, San Diego, CA) and TO-PRO-3 iodide (Life Technologies, Carlsbad, CA) and the percentages of apoptotic cells were determined by flow cytometry. To analyze synergism between, ABT199, decitabine, or cytarabine (AraC) and OTX015, cells were treated with combinations for 48 hours and the percentages of annexin V-positive, apoptotic cells were determined by flow cytometry. The combination index (CI) for each drug combination was calculated by median dose effect and isobologram analyses (assuming mutual exclusivity) utilizing the commercially available software Compusyn<sup>16</sup>. CI values of less than 1.0 represent a synergistic interaction of the two drugs in the combination. The CI values were input into GraphPad V6.0/V7.0 to create the Box and Whisker plots of the range of the CI values for each cell line and combination. The range of CI values for each cell line or primary AML sample does not allow the inference or comparisons of greater or less synergy between other cell lines or primary samples.

**Assessment of percentage non-viable cells.** Following designated treatments, patient-derived AML cells were stained with trypan blue (Sigma, St. Louis, MO). The numbers of non-viable cells were determined by counting the cells that exhibited trypan blue uptake in a hemocytometer, and were reported as a percentage of the untreated control cells. Alternatively, cells were washed with 1X PBS, stained with TO-PRO-3 iodide and analyzed by flow cytometry in the FL-4 fluorescence channel.

**Assessment of leukemia cell differentiation.** Following knockdown of RUNX1 by shRNA in OCI-AML5 and Mono-Mac1 cells, cells were harvested and washed with 1X PBS. Cell were re-suspended in 0.5% BSA/PBS and stained with FITC-conjugated anti-CD86 antibody [RRID:AB\_396012] and APC-conjugated anti-CD11b antibody [RRID:AB\_398456] or FITC-conjugated IgG1 isotype control [RRID:AB\_396090] and APC-conjugated IgG1 isotype control antibody [RRID:AB\_398613] in the

dark, at 4°C for 15-20 minutes. Cells were washed with 0.5% BSA/PBS by centrifugation at 125 x g for 5 minutes, and then re-suspended in 0.5% BSA/PBS for analysis by flow cytometry. Cells were assessed in the FL-1 and FL-4 fluorescence channels. Differentiation of leukemia cells due to RUNX1 shRNA knockdown was also determined by examination of cellular/nuclear morphology. Cells transduced with sh NT or RUNX1 shRNAs were cytopspun onto glass slides at 500 rpm for 5 minutes. The cytopspun cells were fixed and stained with a Protocol® HEMA3 stain set (Fisher Scientific, Kalamazoo, MI). Cellular/nuclear morphology was assessed by light microscopy. Two hundred cells were counted in at least 5 sections of the slide for each condition. The % morphologic differentiation is reported relative to the sh NT-transduced cells. Representative images were captured utilizing a 40X objective lens and a CCD camera attached to the microscope.

**Cell lysis and protein quantitation.** Untreated or drug-treated cells were centrifuged, and the cell pellets were incubated in lysis buffer on ice for 30 minutes, as previously described <sup>17,18</sup>. After centrifugation, an aliquot of each cell lysate was diluted 1:10 and the protein content was quantitated using a BCA protein quantitation kit (Pierce, Rockford, IL), according to the manufacturer's protocol. Protein concentrations were determined by comparing the absorbance at 562 nm compared to a known concentration range of bovine serum albumin (BSA) from 0.125 mg to 2 mg/mL.

**SDS-PAGE and immunoblot analyses.** Seventy five micrograms of total cell lysate were used for SDS-PAGE. Western blot analyses were performed on total cell lysates using specific antisera or monoclonal antibodies. Blots were washed with 1X PBST, then incubated in IRDye 680 goat anti-mouse or IRDye 800 goat anti-rabbit secondary antibodies (LI-COR, Lincoln, NE) for 1 hour, washed 3 times in 1X PBST and scanned with an Odyssey CLX Infrared Imaging System (LI-COR, Lincoln, NE). The expression levels of  $\beta$ -Actin in the cell lysates were used as the loading control for the Western blots. Immunoblot analyses were performed at least twice. Representative immunoblots were subjected to densitometry analysis. Densitometry was performed using ImageJ software <sup>19</sup>.

**Reverse phase protein array analysis.** RPPA was performed in the Functional Proteomics RPPA core facility at the MD Anderson Cancer Center. This array allows the simultaneous detection of 304 unique antibodies against human proteins. This array is curated and highly validated. Briefly, cell lysates were serially diluted two-fold for 5 dilutions (from undiluted to 1:16 dilution) and arrayed on nitrocellulose-coated slides in an 11 x 11 format. Samples were probed with antibodies by tyramide-based signal amplification approach and visualized by DAB colorimetric reaction. Slides were scanned on a flatbed scanner to produce 16-bit tiff image. Spots from tiff images were identified and the density was

quantified by Array-Pro Analyzer. Relative protein expression for each sample were normalized by interpolation of each dilution curves from the "standard curve" (supercurve) of the slide (antibody). Supercurve is constructed by a script in R, written by the Bioinformatics Department at the University of Texas MD Anderson Cancer Center<sup>20</sup>. These values (given as Log2 values) are defined as Supercurve Log2 (Raw) values and imported into an Excel worksheet. All the data points were normalized for protein loading and transformed to linear value, designated as "Normalized Linear" (labeled "NormLinear" in the worksheet). "Normalized Linear" values were transformed to Log2 values (labeled "NormLog2" in worksheet), and then median-centered for hierarchical clustering analysis (labeled "NormLog2\_MedianCentered" in the worksheet). Median-centered values were then formatted for heatmap generation in the "Format for Heatmap" worksheet. Our data were further processed and our heatmaps display only proteins that were altered greater than or equal to 25% up or down and had a p-value of less than 0.05. Multiple hypotheses testing correction was applied using the false discovery rate (fdr) method as implemented in the R statistical system.

**CRISPR/Cas9 editing of the RUNX1 +24 kb enhancer region in OCI-AML5 cells.** To create enhancer malfunction in the RUNX1 +24 kb enhancer region within an intron of the RUNX1 gene, two different locations within the peak that exhibited the highest occupancy of BRD4 were utilized for single guide RNA prediction for CRISPR/Cas9 gene editing. The CCTOP prediction algorithm<sup>21</sup> was utilized to develop single guide RNAs that were ordered as complementary DNA oligos, annealed to each other in high salt buffer and cloned into a lentiviral vector with puromycin selection. A negative control sgRNA was also generated. The pLenti-sgRNA plasmid vector was a gift from Eric Lander & David Sabatini (Addgene plasmid # 71409). The sgRNA-containing vectors were packaged as described above. The packaged vectors/viruses were transduced into OCI-AML5 cells and incubated for 48 hours. Transduced cells were selected with 0.5 µg/mL of puromycin for 1 week. Adenoviral Cas9 was transduced into the cells or recombinant Cas9 was transfected with an Amaxa Nucleofector II device and the cells were grown for 5 days or 10 passages. Following this, total protein lysates were isolated and utilized for immunoblot analysis and other analyses. To determine the mutations generated in the OCI-AML5 cells transduced with guide RNAs and Cas9, we performed PCR amplification and next-generation sequencing. We also downloaded publicly available K562 Transcription Factor ChIP-Seq profiles from the ENCODE project<sup>22</sup>. These profiles were aligned against the CRISPR-mutated sequencing profile utilizing the integrated genome viewer (IGV) software.

**Cell cycle analysis of AML cells.** After the designated treatments, cells were harvested by centrifuging at 125 x g for 5 minutes. Cells were washed twice with 1× phosphate-buffered saline (PBS) in 12 x 75 flow tubes, re-suspended in 200 µL of 1X PBS and fixed in 70% ethanol by adding 800 µL of molecular grade 70% ethanol dropwise to the cells in the tube. The tubes were then vortexed to mix and stored overnight at -20°C. Fixed cells were washed twice with 1× PBS by centrifuging at 125 x g for 5 minutes and then stained in 250 µL of DNA staining buffer [5 mL Triton-PBS (100 µL of Triton X100 in 100 mL of 1X PBS) with 100 µL of 1 mg/mL propidium iodide and 100 µL of 10mg/mL RNase A] in the dark for 15 minutes at 37°C. Cell-cycle data were collected on a flow cytometer with a 488 nM laser in the FL-2 channel and analyzed with Accuri CFlow6 software (BD Biosciences).

**AML xenograft models.** All animal studies were performed under a protocol approved by the IACUC at M.D. Anderson Cancer Center, an AAALAC-accredited institution. To determine the *in vivo* effects of RUNX1 knockdown on leukemia progression and engraftment, 1 million OCI-AML5/GFP-Luc cells transduced with Tet-inducible Runx1 shRNA were injected with a 26 gauge needle into the lateral tail vein of NSG mice (n=7) which had received a pre-conditioning dose of radiation (2.5 gray) 24 hours prior to injection of cells. We also implanted OCI-AML5/GFP-Luc inducible (i)-sh-Runx1 expressing cells that had been treated with 100 ng/ml of doxycycline for 72 hours to induce the shRNA prior to injection into the mice. All the mice were monitored for 7 days and imaged to document engraftment. Following this, mice were treated daily with 10 mg/kg of doxycycline (prepared in sterile water) (daily by oral gavage) for 5 weeks. Mice were injected with 75 mg/kg of D-Luciferin (prepared in 1X PBS and sterile-filtered) and imaged once per week utilizing a Xenogen IVIS *in vivo* imaging system to monitor disease status and treatment efficacy. Mice that became moribund or experienced hind limb paralysis were euthanized according to the approved IACUC protocol. Veterinarians and veterinary staff members assisting in determining when euthanasia was required were blinded to the experimental conditions of the study. The survival of the mice is represented by a Kaplan-Meier survival plot. A Mantel–Cox rank sum test was utilized for comparisons of the efficacy of the different treatment cohorts to the No DOX control. P values of < 0.05 were assigned significance.

To assess the *in vivo* activity of the combination of RUNX1 knockdown by shRNA in combination with OTX015, 0.2 x 10<sup>6</sup> Mono-Mac-1 cells that had been transduced with GFP/Luciferase and separately with DOX-inducible RUNX1 shRNA, were injected into the lateral tail vein of NSG mice (n=7) which had received a pre-conditioning dose of radiation (2.5 gray) 24 hours prior to injection of cells. Mice were monitored for 4 days and imaged utilizing a Xenogen IVIS *in vivo* imaging system to document

engraftment before treatment was initiated. Mice were treated with vehicle, 10 mg/kg of doxycycline (daily by oral gavage) and/or 50 mg/kg of OTX015 (daily x 5 days per week, by oral gavage) for 4 weeks. All mice in each treatment cohort were imaged utilizing a Xenogen IVIS in vivo imaging system once per week to monitor disease status and treatment efficacy. Mice that became moribund or experienced hind limb paralysis were euthanized. Veterinary staff members assisting in determining when euthanasia was required were blinded to the experimental conditions of the study. The survival of the mice is represented by a Kaplan-Meier survival plot. A Mantel–Cox rank sum test was utilized for comparisons of the efficacy of the different treatment cohorts to the vehicle control. P values of < 0.05 were assigned significance.

To assess the *in vivo* activity of BETi OTX015 and BET PROTAC ARV-771,  $2.5 \times 10^6$  luciferase-expressing OCI-AML5 cells (OCI-AML5/GFP-Luc) were injected into the lateral tail vein of NSG mice (n=7) which had received a pre-conditioning dose of radiation (2.5 gray) 24 hours prior to injection of cells. Mice were monitored for 7 days and imaged with a Xenogen IVIS in vivo imaging system to document engraftment before treatment was initiated. Mice were treated with vehicle, 50 mg/kg of OTX015 (daily x 5 days per week, for 3 weeks, by oral gavage) 10 mg/kg ARV-771 or 30 mg/kg of ARV-771 (subcutaneous injection, daily x 5 days per week for 3 weeks). All mice in each treatment cohort were imaged with a Xenogen IVIS in vivo imaging system once per week to monitor disease status and treatment efficacy. Mice that became moribund or experienced hind limb paralysis were euthanized according to the approved IACUC protocol. Veterinary staff assisting in determining when euthanasia was required were blinded to the experimental conditions of the study. The survival of the mice is represented by a Kaplan-Meier survival plot. A Mantel–Cox rank sum test was utilized for comparisons of the efficacy of the different treatment cohorts to the vehicle control. P values of < 0.05 were assigned significance. A separate cohort of mice was injected as above, monitored for 2 weeks prior to treatment initiation. Mice were then treated for one week with vehicle, OTX015 or ARV-771, imaged by bioluminescent imaging on a Xenogen IVIS in vivo imaging system and sacrificed for correlative studies. The bone marrow and spleen from the mice was analyzed for the percentage of GFP-positive cells.

To assess the *in vivo* activity of narciclasine, fenbendazole, and cinobufagin,  $2.5 \times 10^6$  luciferase-expressing OCI-AML5 cells (OCI-AML5/GFP-Luc) were injected into the lateral tail vein of NSG mice which had received a pre-conditioning dose of radiation (2.5 gray) 24 hours prior to injection of cells. Mice were monitored for 7 days and imaged on a Xenogen IVIS in vivo imaging system to document

engraftment before treatment was initiated. Mice were treated with vehicle, 1 mg/kg narciclasine (5 days per week by subcutaneous injection), 50 mg/kg or 100 mg/kg of fenbendazole (5 days per week by oral gavage), or 1 mg/kg of cinobufagin (BID, 5 days per week by subcutaneous injection) for 5 weeks. Mice were imaged on a Xenogen IVIS in vivo imaging system once per week to document treatment efficacy. The survival of the mice is represented by a Kaplan-Meier survival plot. A Mantel–Cox rank sum test was utilized for comparisons of the efficacy of the different treatment cohorts to the vehicle control. P values of < 0.05 were assigned significance.

**Statistical analysis.** Significant differences between values obtained in a population of AML cells treated with different experimental conditions were determined using the Student’s t-test or Kruskal Wallis test in GraphPad V7. For the *in vivo* mouse models, a two-tailed t-test or a Mantel–Cox Rank sum test was utilized for group comparisons. P values of < 0.05 were assigned significance.

**Data and Software availability.** RNA-Seq datasets have been deposited in GEO under Accession number (GSE119261).

## References for Supplemental Materials and Methods

1. Khan M, Cortes J, Kadia T, et al. Clinical Outcomes and Co-Occurring Mutations in Patients with RUNX1-Mutated Acute Myeloid Leukemia. *Int J Mol Sci.* 2017;18(8).
2. Wiederschain D, Wee S, Chen L, et al. Single-vector inducible lentiviral RNAi system for oncology target validation. *Cell Cycle.* 2009;8(3):498-504.
3. Pelish HE, Liao BB, Nitulescu, II, et al. Mediator kinase inhibition further activates super-enhancer-associated genes in AML. *Nature.* 2015;526(7572):273-276.2.
4. Li H, Durbin R. Fast and accurate short read alignment with Burrows-Wheeler transform. *Bioinformatics.* 2009;25(14):1754-1760.
5. Robinson JT, Thorvaldsdottir H, Winckler W, et al. Integrative genomics viewer. *Nat Biotechnol.* 2011;29(1):24-26.
6. Thorvaldsdottir H, Robinson JT, Mesirov JP. Integrative Genomics Viewer (IGV): high-performance genomics data visualization and exploration. *Brief Bioinform.* 2013;14(2):178-192.4.
7. Buenrostro JD, Wu B, Chang HY, Greenleaf WJ. ATAC-seq: A Method for Assaying Chromatin Accessibility Genome-Wide. *Curr Protoc Mol Biol.* 2015;109:21 29 21-29.
8. Schmidl C, Rendeiro AF, Sheffield NC, Bock C. ChIPmentation: fast, robust, low-input ChIP-seq for histones and transcription factors. *Nat Methods.* 2015;12(10):963-965.
9. Loven J, Hoke HA, Lin CY, et al. Selective inhibition of tumor oncogenes by disruption of super-enhancers. *Cell.* 2013;153(2):320-334.

10. Rao SS, Huntley MH, Durand NC, et al. A 3D map of the human genome at kilobase resolution reveals principles of chromatin looping. *Cell*. 2014;159(7):1665-1680.
11. Kim D, Pertea G, Trapnell C, Pimentel H, Kelley R, Salzberg SL. TopHat2: accurate alignment of transcriptomes in the presence of insertions, deletions and gene fusions. *Genome Biol*. 2013;14(4):R36.
12. Trapnell C, Williams BA, Pertea G, et al. Transcript assembly and quantification by RNA-Seq reveals unannotated transcripts and isoform switching during cell differentiation. *Nat Biotechnol*. 2010;28(5):511-515.
13. Smyth GK. Linear models and empirical bayes methods for assessing differential expression in microarray experiments. *Stat Appl Genet Mol Biol*. 2004;3:Article3.
14. Lamb J, Crawford ED, Peck D, et al. The Connectivity Map: using gene-expression signatures to connect small molecules, genes, and disease. *Science*. 2006;313(5795):1929-1935.
15. Subramanian A, Narayan R, Corsello SM, et al. A Next Generation Connectivity Map: L1000 Platform and the First 1,000,000 Profiles. *Cell*. 2017;171(6):1437-1452 e1417.8.
16. Chou TC, Talalay P. Quantitative analysis of dose-effect relationships: the combined effects of multiple drugs or enzyme inhibitors. *Adv Enzyme Regul*. 1984;22:27-55.
17. Wang Y, Fiskus W, Chong DG, et al. Cotreatment with panobinostat and JAK2 inhibitor TG101209 attenuates JAK2V617F levels and signaling and exerts synergistic cytotoxic effects against human myeloproliferative neoplastic cells. *Blood*. 2009;114(24):5024-5033.
18. Fiskus W, Verstovsek S, Manshouri T, et al. Heat shock protein 90 inhibitor is synergistic with JAK2 inhibitor and overcomes resistance to JAK2-TKI in human myeloproliferative neoplasm cells. *Clin Cancer Res*. 2011;17(23):7347-7358.
19. Schneider CA, Rasband WS, Eliceiri KW. NIH Image to ImageJ: 25 years of image analysis. *Nat Methods*. 2012;9(7):671-675.
20. Troncale S, Barbet A, Coulibaly L, et al. NormaCurve: a SuperCurve-based method that simultaneously quantifies and normalizes reverse phase protein array data. *PLoS One*. 2012;7(6):e38686.
21. Stemmer M, Thumberger T, Del Sol Keyer M, Wittbrodt J, Mateo JL. CCTop: An Intuitive, Flexible and Reliable CRISPR/Cas9 Target Prediction Tool. *PLoS One*. 2015;10(4):e0124633.
22. Consortium EP. An integrated encyclopedia of DNA elements in the human genome. *Nature*. 2012;489(7414):57-74.

## Supplemental Figure Legends

**Figure S1. Age, RUNX1 mutation status and co-occurring mutations significantly affect survival in AML patients.** **A.** AML status and RUNX1 mutation in 655 patients from the M.D. Anderson AML dataset. **B.** Mutations co-occurring with mtRUNX1 in the M.D. Anderson AML dataset. **C.** Circos plot representation of mutations co-occurring with RUNX1 mutation in the 141 mtRUNX1 expressing AML patient samples in the MD Anderson AML dataset. The width of the ribbon in the inner circle indicates the number of mutations for each gene co-occurring with mtRUNX1. Ribbons connecting mutated genes (labeled on the outer ring) indicate co-mutation with each other and with mtRUNX1. The width of the ribbon between two genes indicates the number of co-occurrences between the co-mutated genes. **D.** Kaplan-Meier survival curve of AML patients based on age and RUNX1 mutation. Younger patients with no RUNX1 mutation have significantly improved survival compared to the other cohorts ( $p < 0.001$ ). **E.** Oncoplot of cultured OCI-AML5, Mono-Mac-1, OCI-AML2, THP1 and HEL92.1.7 cells as well as the primary patient-derived mtRUNX1-expressing AML samples utilized in these studies. GL1-3 are germline mtRUNX1 expressing AML samples. FPD1-3 are germline mtRUNX1 familial platelet disorder samples. **F.** Site of RUNX1 mutations in the cultured and PD, CD34+ AML cells utilized in these studies. **G.** Schematic of the RUNX1b gene indicating the location of the mutations in Mono-Mac-1 and OCI-AML5 as well as the binding sites of the two RUNX1 shRNAs utilized in these studies. **H.** Oncoplot of wtRUNX1 expressing PD, CD34+ AML cells utilized in these studies.

**Table S1. Locations of RUNX1 mutations in the 141 mtRUNX1-expressing AML patients in the MD Anderson AML dataset.**

**Figure S2. RUNX1 depletion by shRNA depletes RUNX1 target gene expression and induces myeloid differentiation in mtRUNX1-expressing AML cells.** **A.** RPPA analysis conducted on OCI-AML5 cells transduced with sh NT or RUNX1 shRNA for 72 hours. Heatmap shows proteins that were up and downregulated  $\geq 25\%$  relative to the sh NT-transduced cells and with a  $p$ -value  $< 0.05$ . The table shows selected protein expressions altered by depletion of RUNX1 and their corresponding  $p$ -value. **B.** OCI-AML5 cells were transduced as previously described for 72 hours. Following this, cells were stained for myeloid differentiations markers CD11b and CD86 by flow cytometry. Columns represent the mean of three experiments  $\pm$  S.E.M. (\* =  $p < 0.05$  relative to sh NT). **C-D.** Morphologic differentiation of OCI-AML5 cells transduced with sh NT or RUNX1 shRNA for 96 hours. Original magnification is 40X. **E-F.** Mono-Mac-1 cells were transduced with sh-NT or RUNX1 shRNA for 72-96 hours. **E.** (inset) Immunoblot analysis was conducted for RUNX1 expression levels in the cell lysates. The expression levels of  $\beta$ -Actin in the lysates served as the loading control. The % of annexin-V positive, apoptotic Mono-Mac-1 cells after RUNX1 shRNA transduction. **F.** Mono-Mac-1 cells transduced as indicated were stained for myeloid differentiations markers CD11b and CD86 by flow cytometry. **G.** HEL92.1.7, OCI-AML2, and THP1 cells were transduced with sh NT or RUNX1 shRNA for 72 hours. Total RNA was isolated and qPCR was performed for RUNX1. The relative mRNA expression was normalized to GAPDH. **H.** HEL92.1.7, OCI-AML2 and THP1 cells were transduced with sh-NT or RUNX1 shRNA for 72 hours. Immunoblot analysis was conducted for RUNX1 in the cell lysates. The expression levels of  $\beta$ -Actin in the lysates served as the loading control. **I.** HEL92.1.7 and THP1 cells were transduced with sh NT or RUNX1 shRNA for 72 hours. At the end of treatment, the % of annexin-V positive, apoptotic cells were determined. **J.** Total cell number of OCI-AML2 cells following transduction with sh NT or RUNX1 shRNA for 72 hours. **K.** OCI-AML2 cells were

transduced with sh NT or RUNX1 shRNA for 72 hours. Then, the cells were stained for myeloid differentiations markers CD11b and CD86 and analyzed by flow cytometry. n.s. = values not significantly different in RUNX1 shRNA transduced versus sh NT transduced cells. **Doxycycline inducible depletion of RUNX1 downregulates target gene expressions.** L. OCI-AML5 i-sh-RUNX1 cells were treated with the indicated concentrations of doxycycline (DOX) for 72 hours. Total RNA was isolated, reverse transcribed and qPCR analysis was performed. The relative mRNA expression of RUNX1, MYC, SPI1/(PU.1), and MPO (normalized against GAPDH) is shown. (\* =  $p < 0.05$  relative to no-Dox cells).

**Figure S3. Treatment with BET inhibitor reduces BRD4 occupancy on the enhancers of RUNX1 in AML MOLM14 cells and alters RUNX1 promoter and enhancer interactions in mtRUNX1 expressing OCI-AML5 cells.** **A.** We utilized publicly available ChIP Seq- data for BRD4 in AML cells (MOLM14) with and without treatment with a BET inhibitor (IBET-151). ChIP-Seq analysis of BRD4 showed broad and high level occupancy at 4 distinct regions along the RUNX1 gene. **B.** Heat map of Hi-C interaction scores within the RUNX1 TAD region in K562 cells shows triangle-shaped regions of high interaction scores. Convergent CTCF sites in the TAD boundaries anchor a loop that separates the RUNX1 TAD from other TADs. **C.** Alignment of the human P2 proximal enhancer with the mouse +110 enhancer reported by Marsman et al., 2017. **D.** Schematic representation of the luciferase-expressing reporter construct generated and utilized in these studies. The luciferase reporter vector contains the P2 promoter (for RUNX1b), +24 kb enhancer in the first intron of RUNX1, or the P2 promoter and the +24 kb enhancer. The enhancer regulatory element was cloned downstream of the luciferase gene. **E.** ChIP qPCR of BRD4, c-Myc, p300, PU.1 and pSer2-RNAP2 occupancy in the RUNX1 +24 kb enhancer following knockdown of BRD4 by shRNA for 72 hours in OCI-AML5 cells. **F.** Relative mRNA expression of BRD4, MYC, and RUNX1 in OCI-AML5 cells transduced with non-targeting shRNA or BRD4 shRNA and incubated 72 hours. Relative expression of each mRNA was normalized to GAPDH. **G.** Colony growth of OCI-AML5 cells transduced with sh-NT or BRD4 shRNA for 72 hours. (\*\*\*\* =  $p < 0.001$  relative to sh-NT).

**Figure S4. Treatment with BET inhibitor JQ1 or BET-PROTAC ARV-771 but not the inactive stereoisomer R-JQ1 or ARV-766 reduces expression of RUNX1 and its target genes in mtRUNX1 AML cells and treatment with PROTACs induces cell death of PD, CD34+ mtRUNX1 AML cells but not normal CD34+ cells.** **A.** Percent apoptosis in Mono-Mac-1 and OCI-AML5 cells treated with the indicated concentrations of BET-PROTAC ARV-825 for 48 hours. The  $IC_{50}$  dose of ARV-825 in each cell line is shown. **B.** OCI-AML5 cells were treated with 250 nM ARV-771 or ARV766 for 48 hours. Then, the % of annexin V-positive, apoptotic cells were determined by flow cytometry. **C.** OCI-AML5 cells were treated with JQ1 or the inactive isomer, R-JQ1 for 18 hours. Then, total cell lysates were prepared and immunoblot analysis was conducted as indicated. The expression levels of  $\beta$ -Actin in the lysates served as the loading control. **D.** OCI-AML5 cells were treated with ARV-771 or the inactive isomer, ARV-766 for 18 hours. Then, total cell lysates were prepared and immunoblot analysis was conducted as indicated. The expression levels of  $\beta$ -Actin in the lysates served as the loading control. **E.** Patient-derived (PD), CD34+ mtRUNX1-expressing AML cells (n=8) and normal CD34+ cells (n=3) were treated with the indicated concentrations of ARV-825 or OTX015 for 48 hours. Following this, the % of propidium iodide-positive, non-viable cells was determined by flow cytometry. **F.** Patient-derived (PD), CD34+ mt RUNX1 AML cells (n=5) and normal CD34+ cells from cord blood (n=3) were treated with the indicated concentrations of ARV-771 for 48 hours. At the end of treatment, cells were stained

with propidium iodide (PI) and the % of PI-positive, non-viable cells were determined by flow cytometry. **G.** % GFP positive cells in the spleen of mice sacrificed after 1 week of treatment with OTX015 or ARV-771 as indicated. \* indicates % GFP-positive cells that were significantly less in the OTX015 and ARV-771-treated mice compared to the vehicle-treated mice ( $p < 0.05$ ).

**Figure S5. BET inhibitor-based combinations exert synergistic lethal activity against mtRUNX1 expressing AML cells.** **A.** OCI-AML5, Mono-Mac-1 and PD CD34+ mtRUNX1 AML cells ( $n=6$ ) were treated with OTX015 (dose range: 250-1000 nM) and ABT-199 (dose range: 10-100 nM) for 48 hours. Then, the % of annexin V-positive, apoptotic cells (OCI-AML5, Mono-Mac-1) or propidium iodide-positive, non-viable cells (PD CD34+ AML cells) was determined by flow cytometry. Median dose effect and isobologram analyses were performed utilizing CompuSyn, assuming mutual exclusivity. Combination index (CI) values less than 1.0 indicate a synergistic interaction of the two agents in the combination. **B.** OCI-AML5, Mono-Mac-1, MOLM13 and MV4-11 cells were treated with OTX015 (dose range: 250-1000 nM) and decitabine (dose range: 250-1000 nM) for 48 hours. At the end of treatment, the % of annexin V-positive, apoptotic cells were determined by flow cytometry. Combination index values were calculated utilizing CompuSyn. Combination index (CI) values less than 1.0 indicate a synergistic interaction of the two agents in the combination. **C.** OCI-AML5 and Mono-Mac-1 cells were treated with OTX015 (dose range: 250-1000 nM) and cytarabine (AraC) (dose range: 250-1000 nM) for 48 hours. At the end of treatment, the % of annexin V-positive, apoptotic cells were determined by flow cytometry. Combination index values were calculated utilizing CompuSyn. Combination index (CI) values less than 1.0 indicate a synergistic interaction of the two agents in the combination. **D.** Drug doses, fractional effects and corresponding combination index values for OTX015 and decitabine in the four cell lines shown in panel **B.**

**Figure S6. CRISPR/Cas9-mediated disruption of the RUNX1 +24 kb enhancer depletes RUNX1 expression, attenuates cell proliferation, induces markers of myeloid differentiation and apoptosis as well as decreases colony growth of OCI-AML5 cells.** **A.** Immunoblot analysis of OCI-AML5 sg Neg or sg+24 kb enhancer-transduced cells 5 days post transfection with recombinant Cas9 protein. The expression levels of  $\beta$ -Tubulin in the lysates served as the loading control. **B.** Cell proliferation of OCI-AML5 sg Neg or sg+24 kb enhancer-transduced cells 3 and 5 days post transfection with recombinant Cas9 protein. **C.** OCI-AML5 sg Neg or sg+24 kb enhancer-transduced cells were stained for myeloid differentiations markers CD11b and CD86 by flow cytometry 5 days post transfection with recombinant Cas9 protein. (\*=  $p < 0.05$  relative to sg Neg-transduced cells). **D.** Morphologic differentiation of OCI-AML5 sg Neg or sg+24 kb enhancer-transduced cells 5 days post transfection with recombinant Cas9 protein. (\*=  $p < 0.05$  relative to sg-Neg transduced cells). **E.** Five days post Cas9 transfection, the % of annexin V-positive, apoptotic OCI-AML5 sg Neg or sg+24 kb enhancer-transduced cells were determined by flow cytometry. (\*\*=  $p < 0.01$  relative to sg Neg-transduced cells) **F.** Colony growth of OCI-AML5 sg Neg or sg+24 kb enhancer-transduced cells plated in methocult media five days post Cas9 transfection and incubated for 7-10 days. (\*\*\*=  $p < 0.005$  relative to sg Neg-transduced cells). Original magnification of representative colonies (4X).

**Figure S7. Gene sets altered by depletion of RUNX1 in mtRUNX1 AML cells.** OCI-AML5 cells were transduced with sh NT or RUNX1 shRNA for 72 hours. RNA-Seq analysis was performed. **A.** The 50 most upregulated and downregulated mRNA expressions and their associated log2 fold changes in RUNX1 shRNA transduced AML cells are shown. **B.** Relative mRNA expression of RUNX1, GLI2,

GATA2, ITGAM (CD11b) and P2RY14 in OCI-AML5 cells transduced with sh NT or RUNX1 shRNA for 72 hours. Expression of each mRNA was normalized to GAPDH.

**Table S2. Overlap in the gene expression signatures in cells treated with ARV-825 or OTX-015 compared to RUNX1 shRNA. A-B.** The fold-change in expression shown is relative to control cells or sh NT in the case of RUNX1 shRNA. Overlapping genes were identified as being up or downregulated in the same direction in the 3 datasets utilizing Excel.

**Figure S8. Treatment with BET-PROTAC causes greater and more sustained depletion of BRD4 and target gene expressions than treatment with OTX015 in mtRUNX1-expressing AML cells. A.** OCI-AML5 cells were treated with the indicated concentrations of ARV-825 or OTX015 for 18 hours. At the end of treatment, total cell lysates were prepared and immunoblot analyses were conducted. The expression levels of  $\beta$ -Actin in the lysates served as the loading control. **B.** OCI-AML5 cells were treated with the indicated concentrations of ARV-825 or OTX015 for 24 hours. One half of the cells were collected and flash frozen. The remaining cells were washed free of the drug and re-plated in fresh media for 24 hours. Following this, cells were harvested and total cell lysates were prepared and immunoblot analyses were conducted. The expression levels of  $\beta$ -Actin in the lysates served as the loading control. **C.** PD, CD34+ AML cells were treated with the indicated concentrations of ARV-825 or OTX015 for 18 hours. At the end of treatment, total cell lysates were prepared and immunoblot analyses were conducted. The expression levels of  $\beta$ -Actin in the lysates served as the loading control.

**Table S3. List of expression mimickers (EMs) with expression signatures matching knockdown of RUNX1 in mtRUNX1 AML cells.** The RNA-Seq expression signature of RUNX1 knockdown in OCI-AML5 cells was compared to the expression signatures in the LINCS1000-CMap database. A rank ordered list of the top 45 chemical agents matching the RNA expression signature of RUNX1 knockdown is presented.

**Figure S9. Treatment with anisomycin, cinobufagin, narciclasine and fenbendazole induces apoptosis of mutant RUNX1 cells and reduces leukemia burden in NSG mice engrafted with OCI-AML5/GFP-Luc cells. A.** Mono-Mac-1 cells were treated with the indicated concentrations of anisomycin, cinobufagin or narciclasine for 48 hours. Following this, the % of annexin V-positive apoptotic cells was determined by flow cytometry. **B.** OCI-AML5 cells were treated with the indicated concentrations of anisomycin, cinobufagin or CD1530 for 8 hours. Total RNA was extracted, purified and reverse transcribed. The resulting cDNA was utilized for qPCR analysis as indicated. The relative mRNA expression of each target is normalized to the expression of GAPDH and compared to the control cells. **C.** NSG mice were implanted with luciferase-expressing OCI-AML5 cells and monitored for 4-7 days. Mice were imaged to document engraftment of leukemia and then treated with vehicle, 1 mg/kg of narciclasine, 50 mg/kg or 100 mg/kg of fenbendazole or 1 mg/kg of cinobufagin (BID) as indicated. At the end of treatment, mice were imaged with a Xenogen camera and total photon counts were recorded. \* indicates bioluminescent values that are significantly less in EM-treated mice compared to vehicle-treated mice ( $p < 0.05$ ).

**Figure S10. Treatment with high dose etoposide but not cytarabine (AraC) induced apoptosis and attenuated c-Myc and c-Myb expression in mtRUNX1-expressing AML cells. A.** OCI-AML5 cells were treated with etoposide and AraC (dose range: 100-2500 nM) for 48 hours. At the end of treatment, the % of annexin V-positive, apoptotic cells were determined by flow cytometry. **B.** OCI-AML5 cells

were treated with the indicated concentrations of AraC or etoposide for 24 hours. Immunoblot analyses were conducted. The expression levels of  $\beta$ -Actin in the lysates served as the loading control.

**Table S4. Oligonucleotide primers utilized in these studies.** The sequences of the primers are listed in 5' - to 3' orientation.

Figure S1

A

AML Status	mtRUNX1+	mtRUNX1-	Total
De novo	84 (60%)	397	481
Prior MDS +/- MPD	47 (33%)	96	143
Prior MPN	10 (7%)	21	31
<b>Total</b>	<b>141</b>	<b>514</b>	<b>655</b>

B

Mutations co-occurring with mtRUNX1 in AML	N (Out of a total of 141)	% of mtRUNX1 pts
ASXL1	44	31.2
FLT3-ITD	34	24.1
TET2	25	17.7
DNMT3	23	16.3
IDH1	20	14.2
IDH2	18	12.8
NRAS	18	12.8
PTPN11	10	7.1
CEBPA	9	6.4
FLT3-D835	8	5.7
JAK2	8	5.7
TP53	8	5.7
WT1	8	5.7
EZH2	7	5.0
KRAS	5	3.5
KIT	5	3.5
GATA2	4	2.8
NPM1	3	2.1
AML1-ETO	1	0.8

D

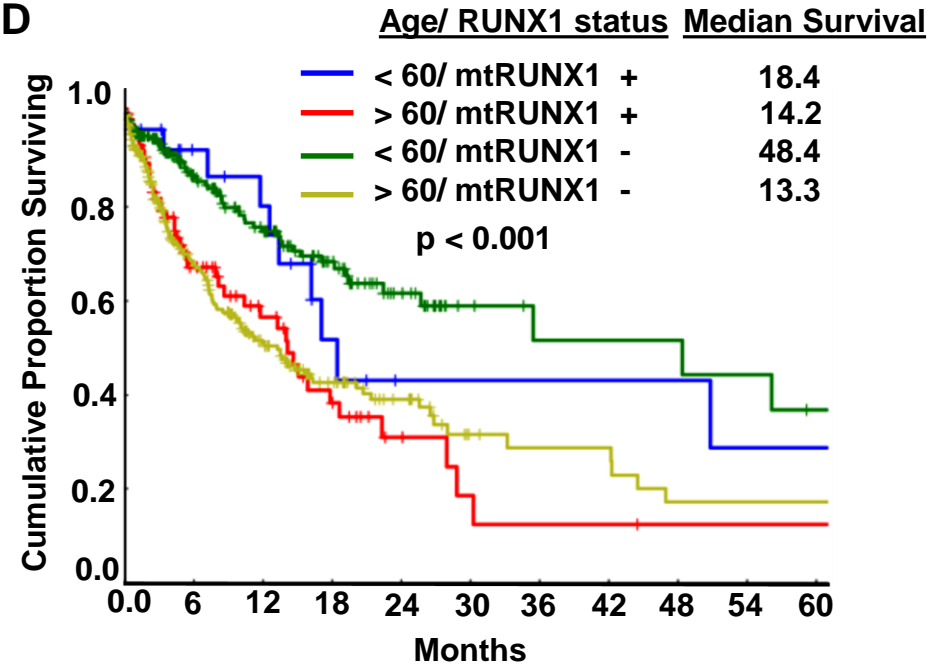


Figure S1

C

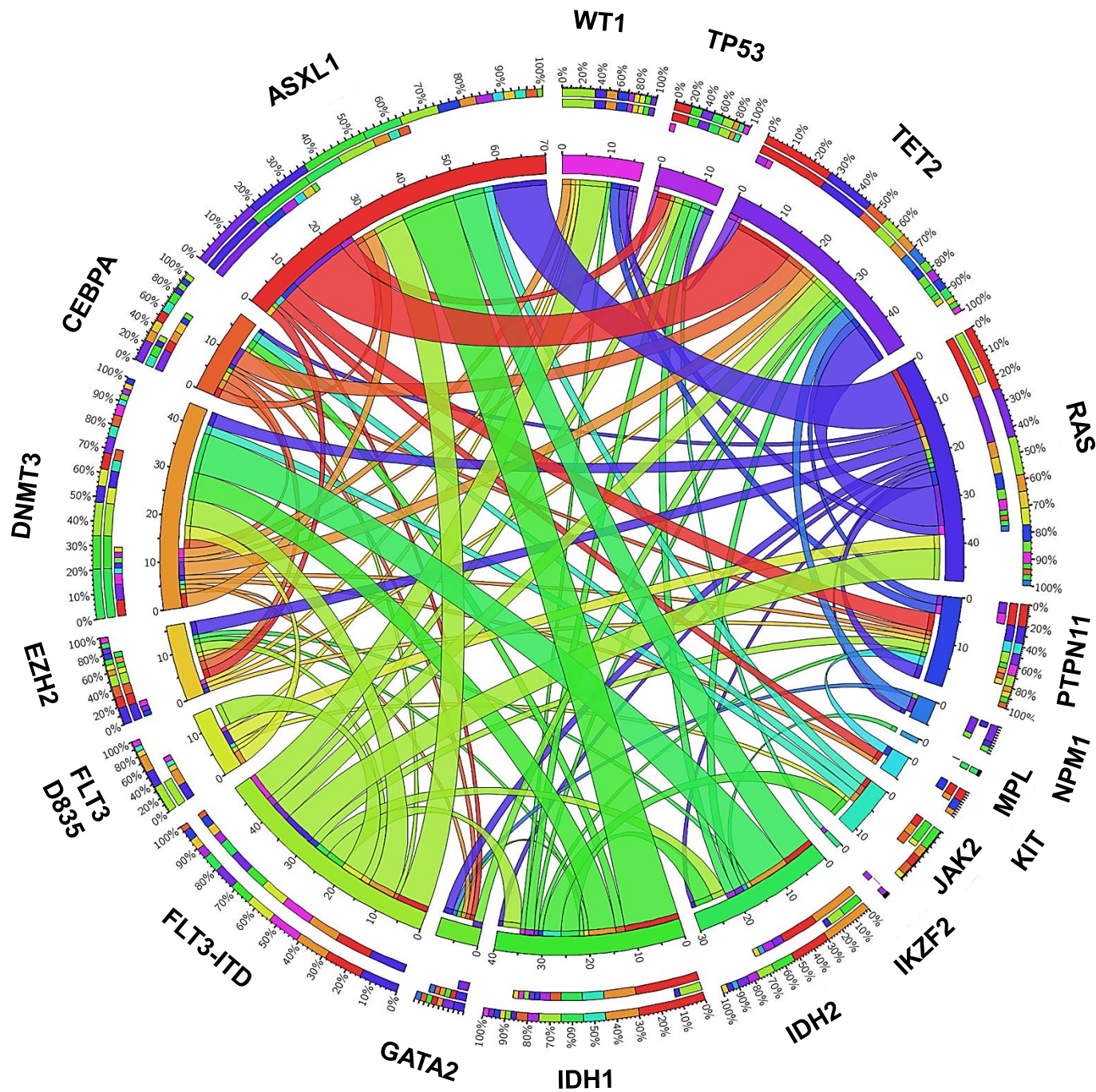




Figure S1

E

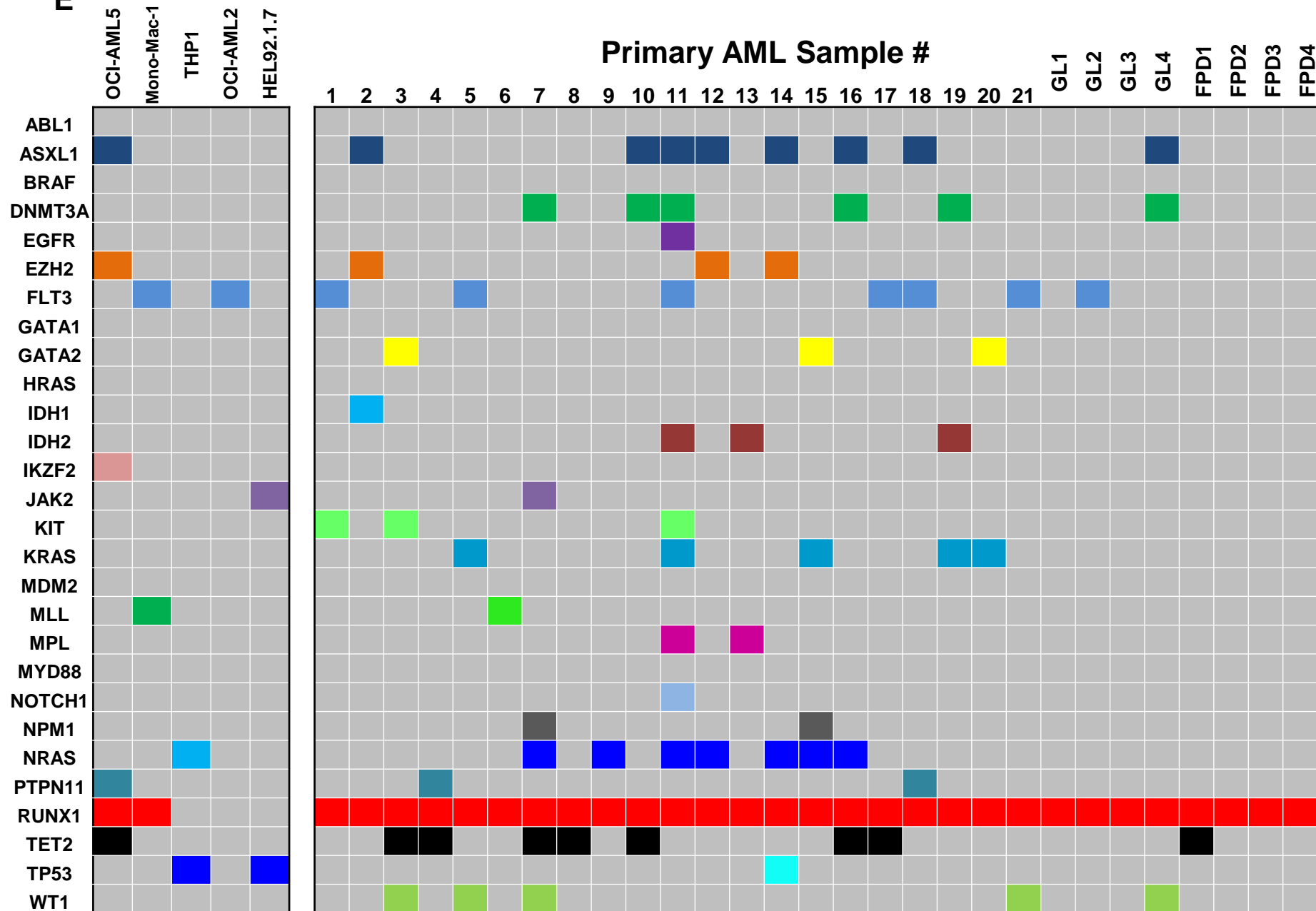


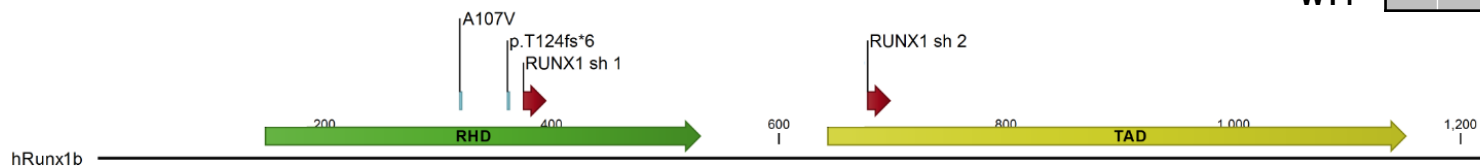
Figure S1

**F**

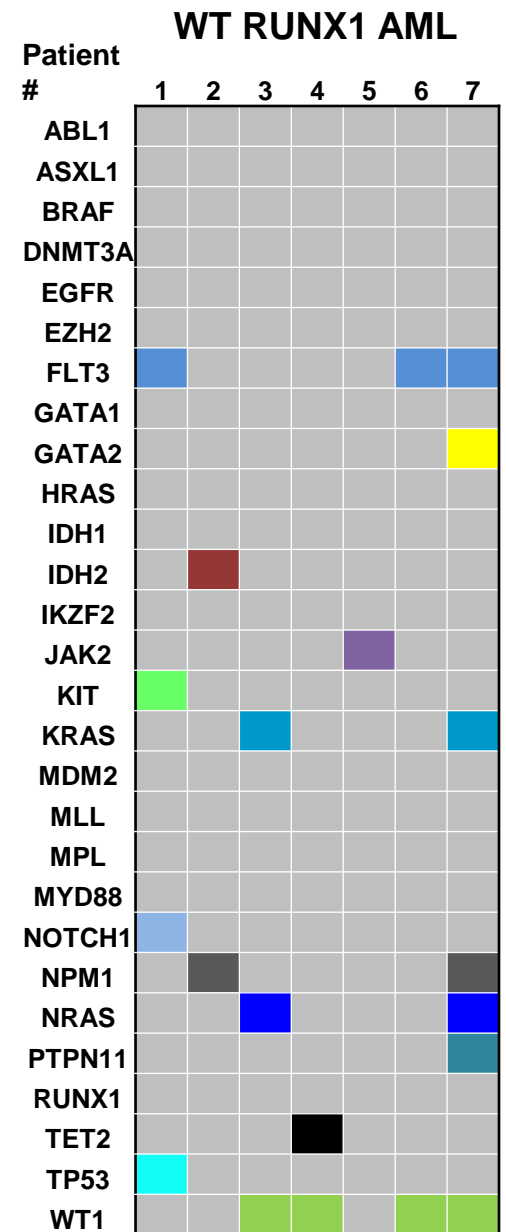
Cell line	Mutation in RUNX1 DNA	Protein Change
OCI-AML5	c.370_371 insTGCTA	p.T124fs*6
Mono-Mac-1	c. 321G>A	p.A107V

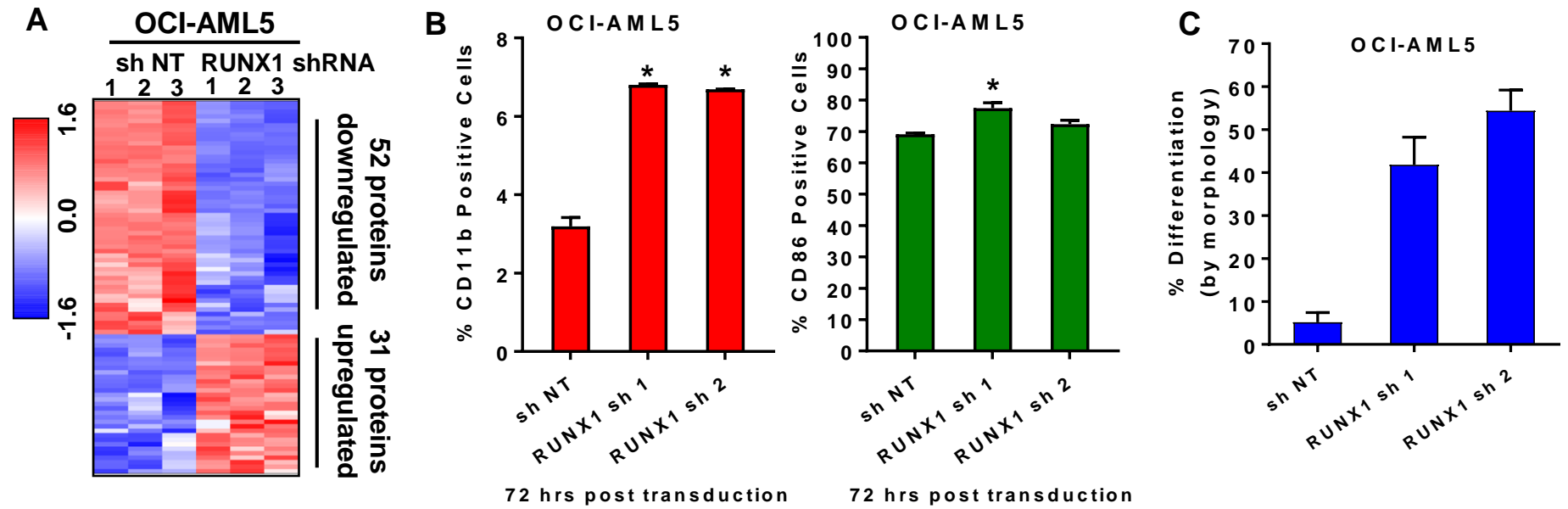
PD AML Number	Mutation in RUNX1 DNA	Protein Change
1	c.749-755 del	p.R250fs
2	c.299C>T	p.S100F
3	c.937dupC	p.L313fs
4	c.496C>T	p.R166*
5	c.601C>T; c.1268_1269del	p.R201*; pR423fs
6	c.493G>T; c.1011delC	p.G165C; pA338fs
7	c.236dupT	p.E80fs
8	c.496C>T	p.R166*
9	c.302dupT	p.L102fs*36
10	c.385_386insG	p.L129fs*9
11	c.510+1_510+2insAGG	unknown
12	c.1096_1103del	p.I366fs
13	c.1244_1250dupAGTTCTC	p.M418fs
14	c.601C>T	p.R201*
15	c.1348_1354dupAGCACG	p.V452fs*
16	c.987_988dupGT; c900_901insTCCG	p.F330fs*265; p.P301fs*300
17	c.601C>T	p.R201*
18	c.238dupG	p.E80fs*58
19	c.592G>A	p.D198N
20	c.502G>A	p.G168R
21	c.167T>C	p.L56S

**G**



**H**





Protein Target	Log2 fold change (RUNX1sh/sh NT)	P-value
pRb (S807/811)	-2.71	0.0005
MYC	-1.13	0.0022
BCL2	-0.79	0.0006
NOTCH1	-0.55	0.01
Cl Caspase 7	0.43	0.0011
p27 KIP	0.61	0.0067

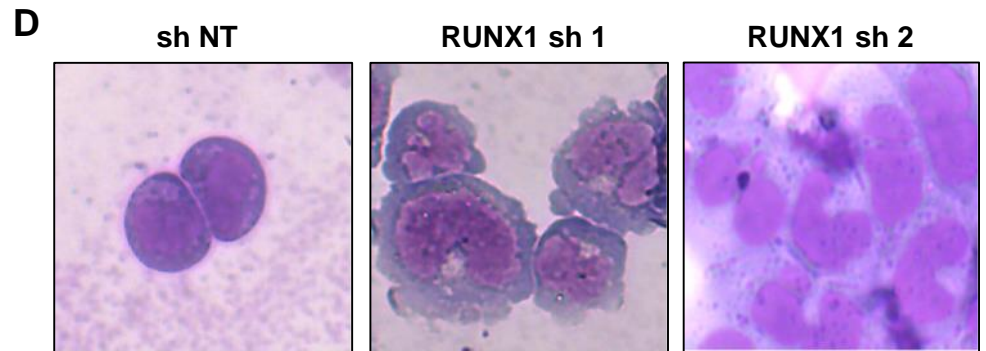


Figure S2

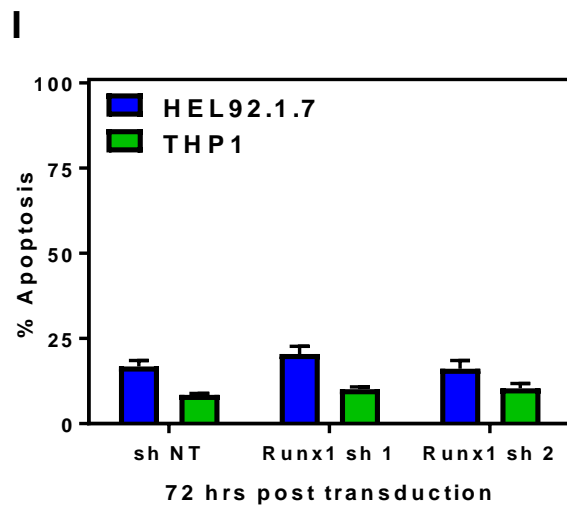
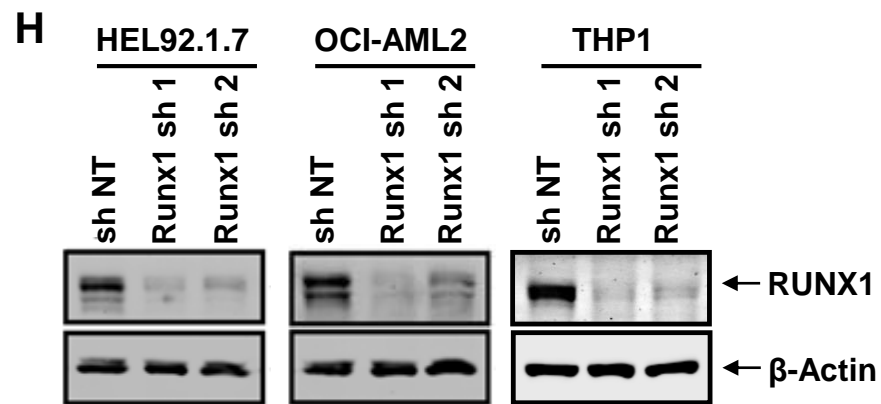
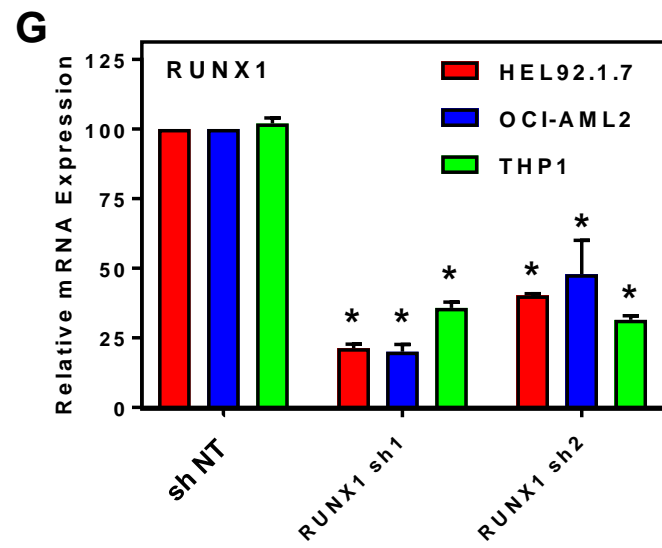
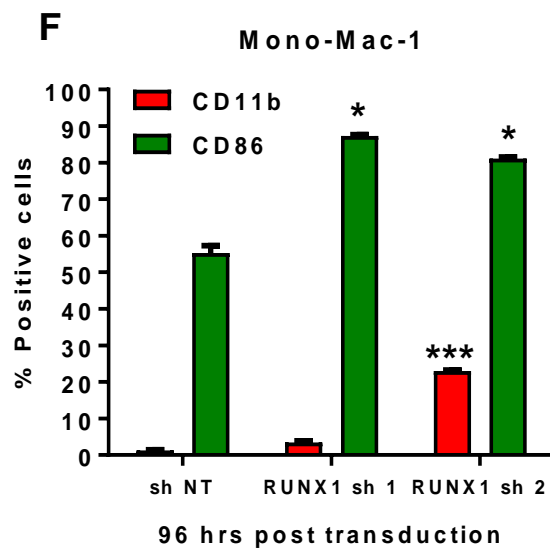
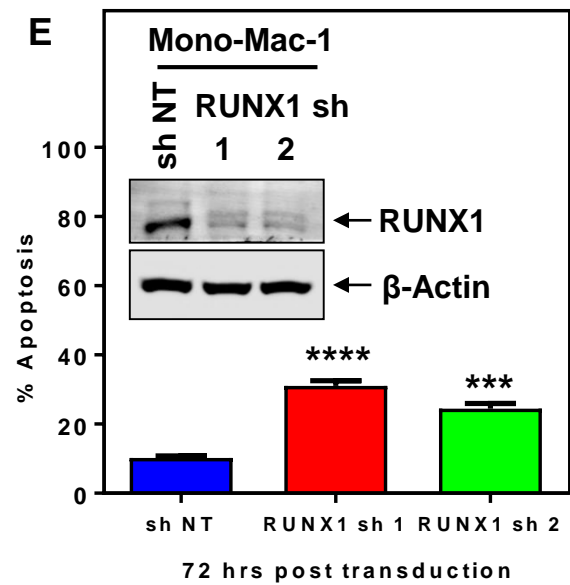


Figure S2

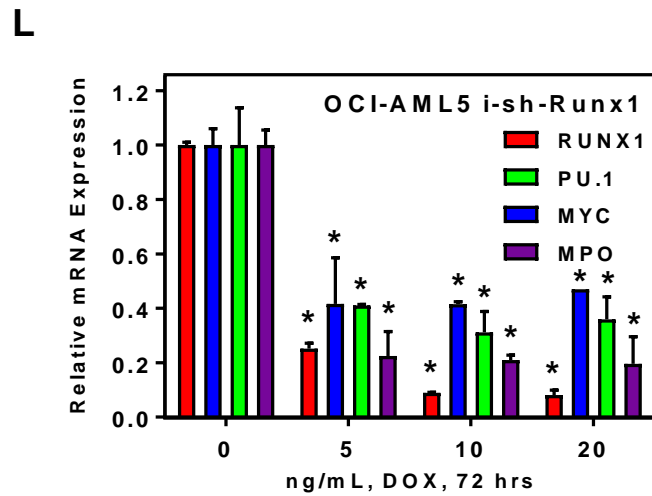
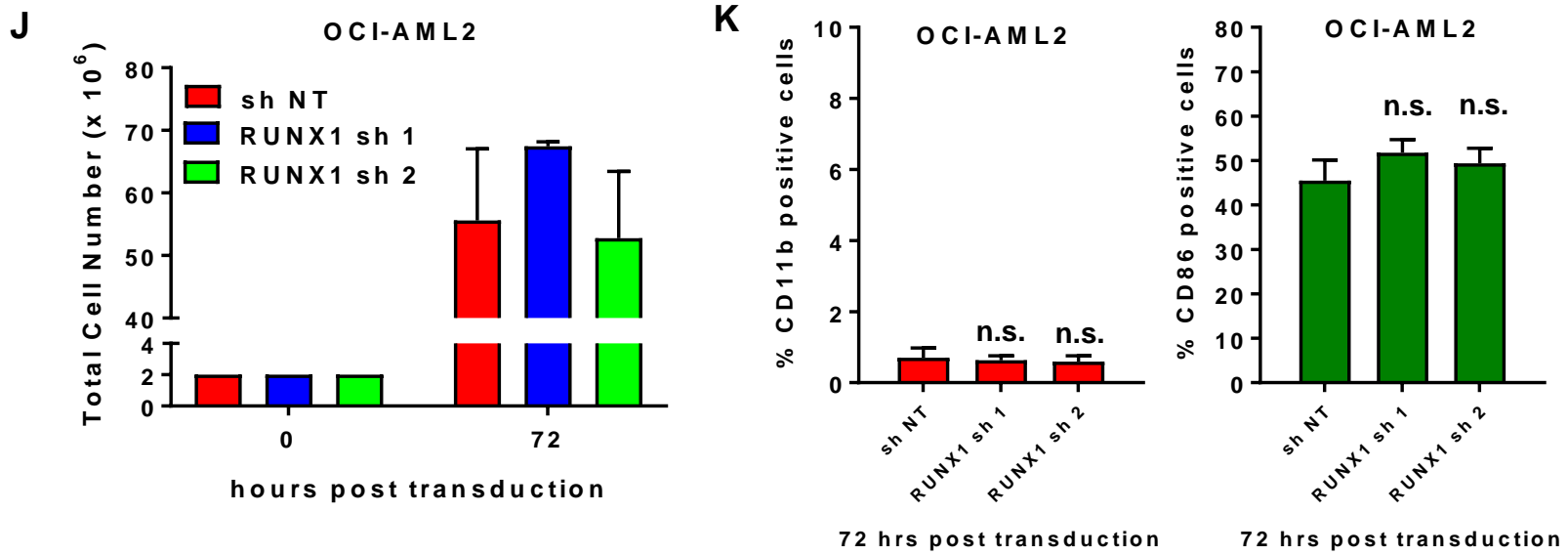
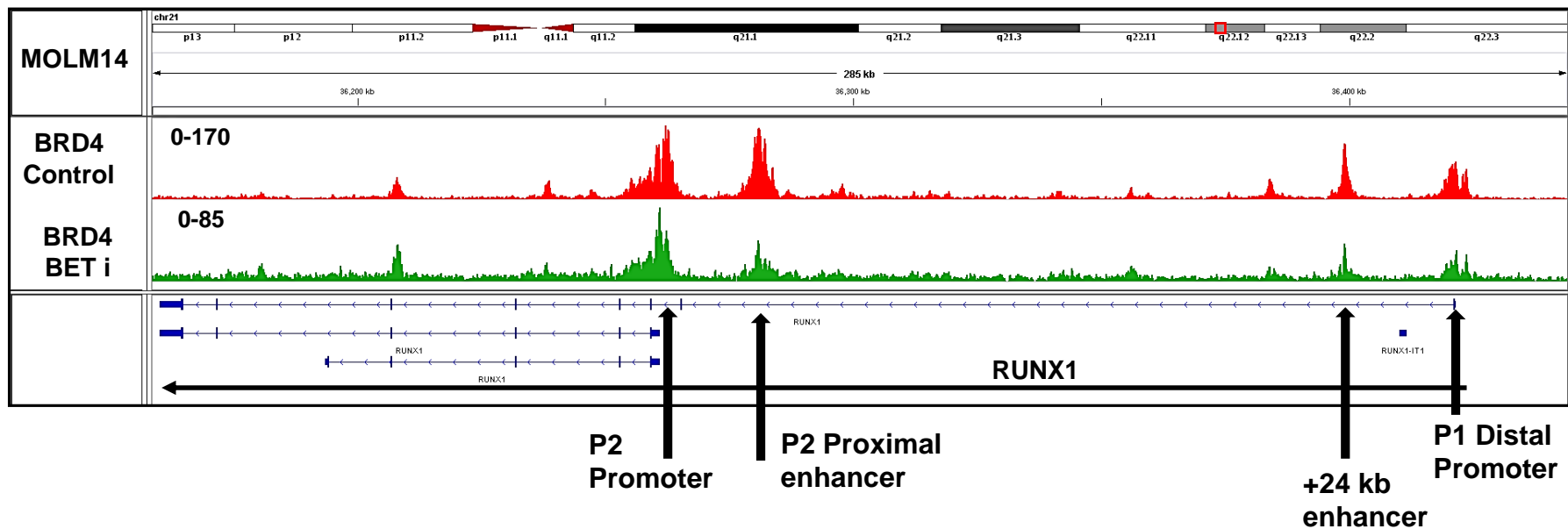


Figure S2

A



B

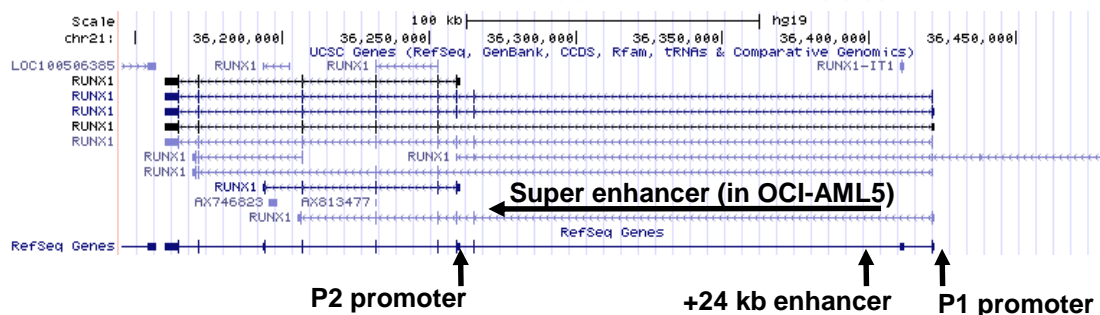
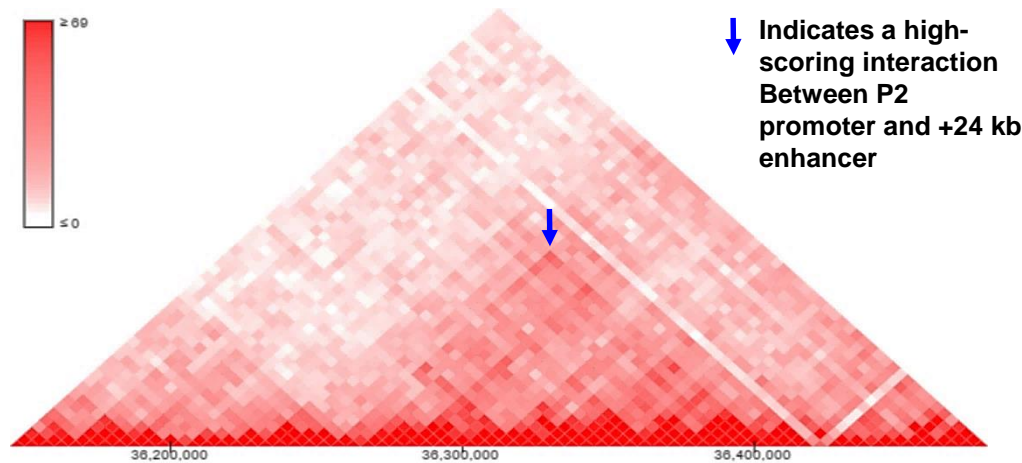


Figure S3



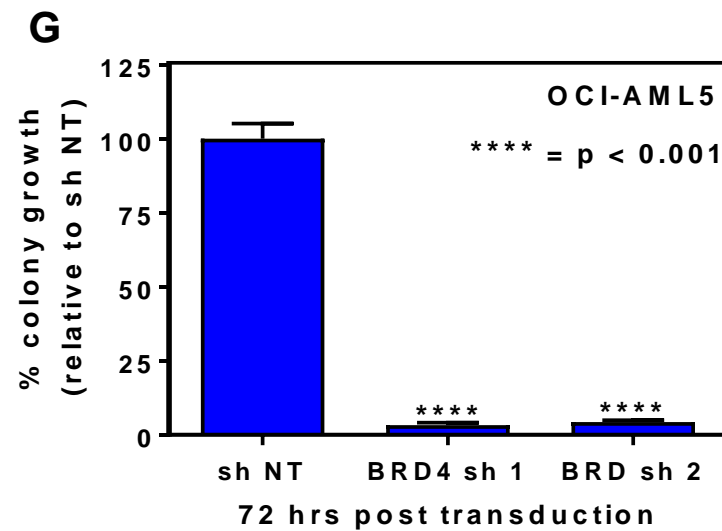
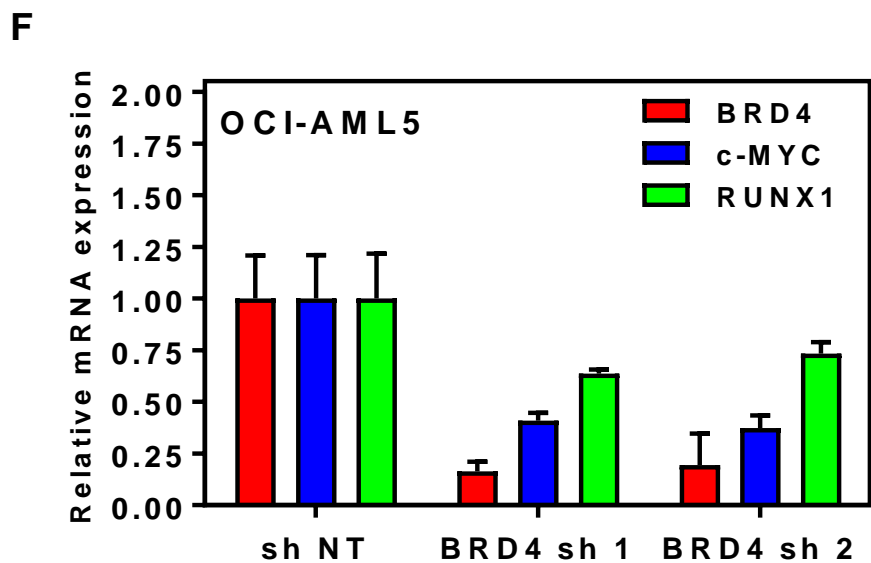
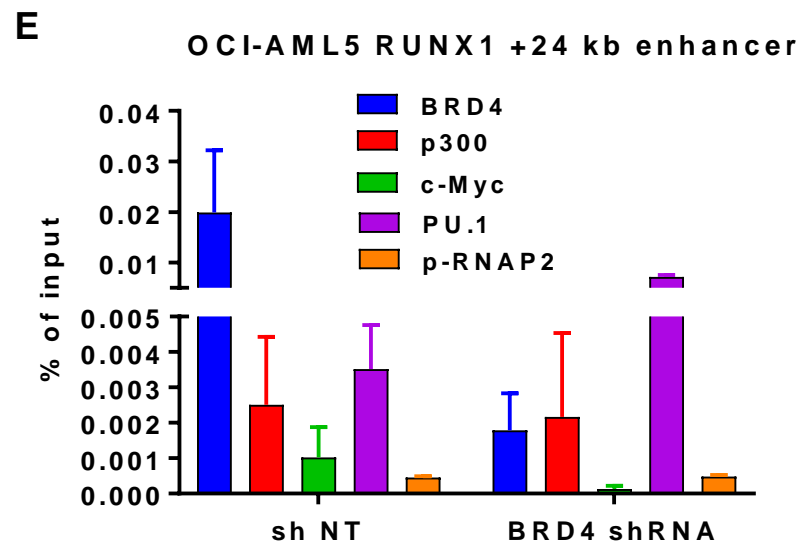
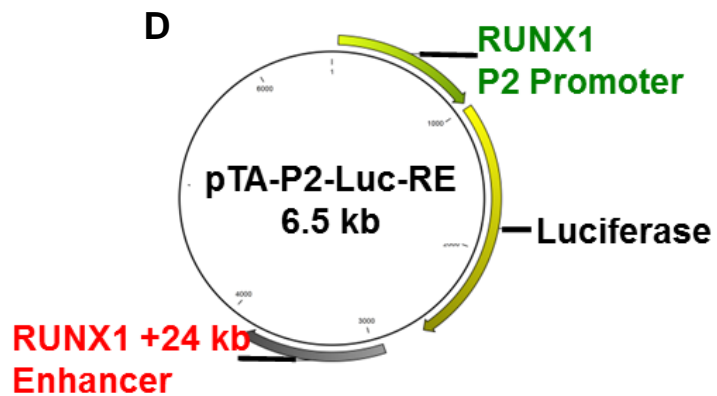
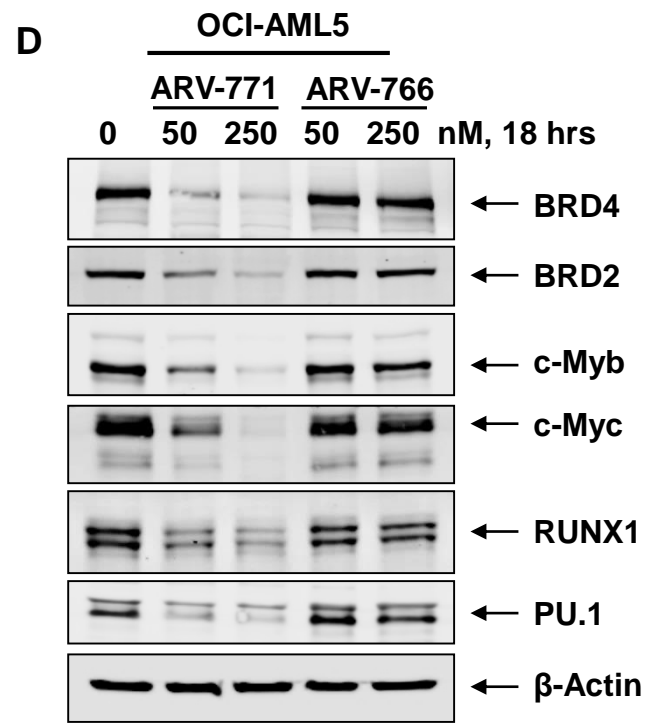
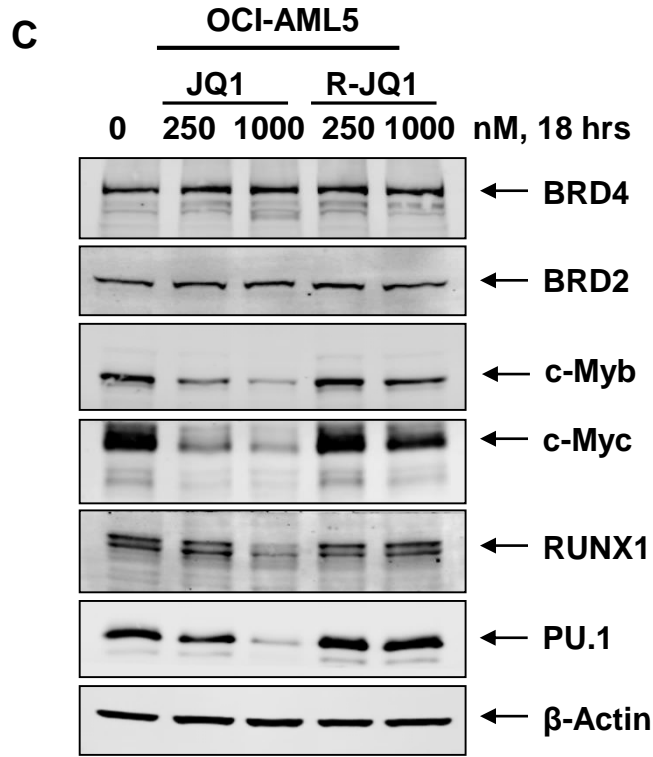
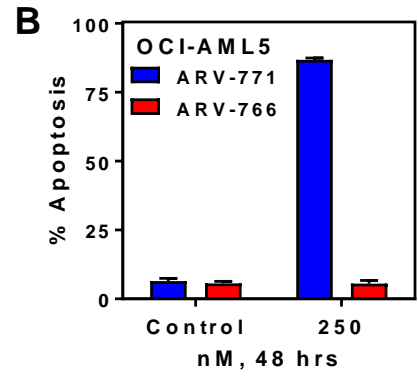
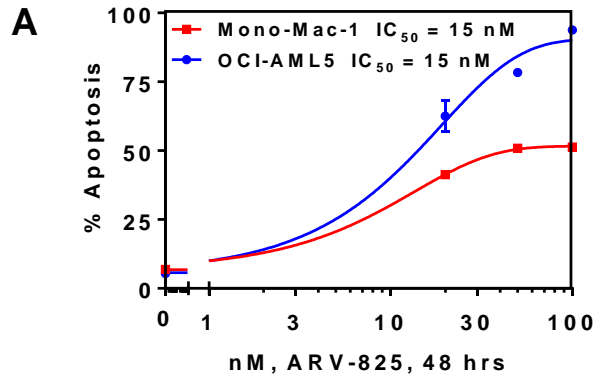
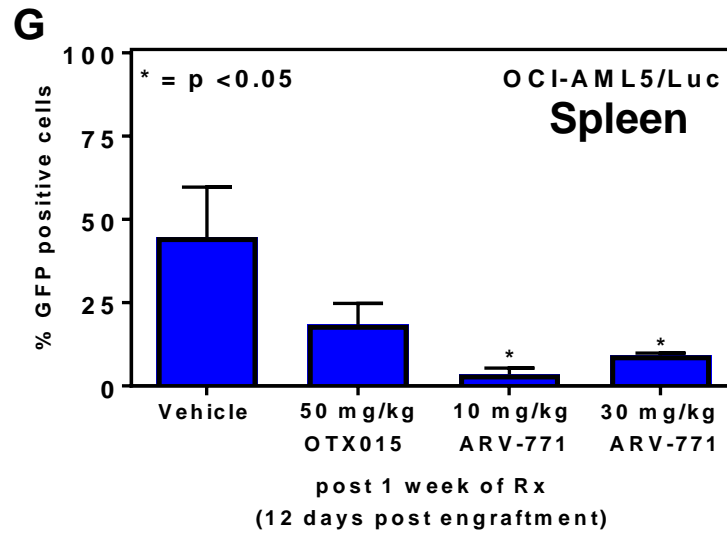
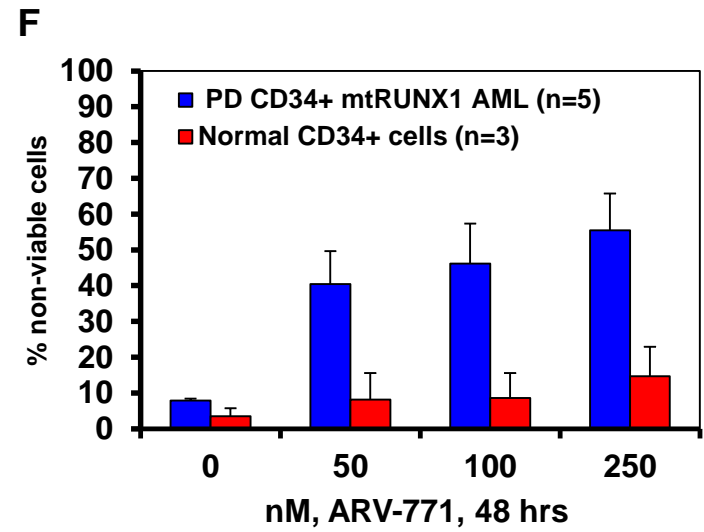
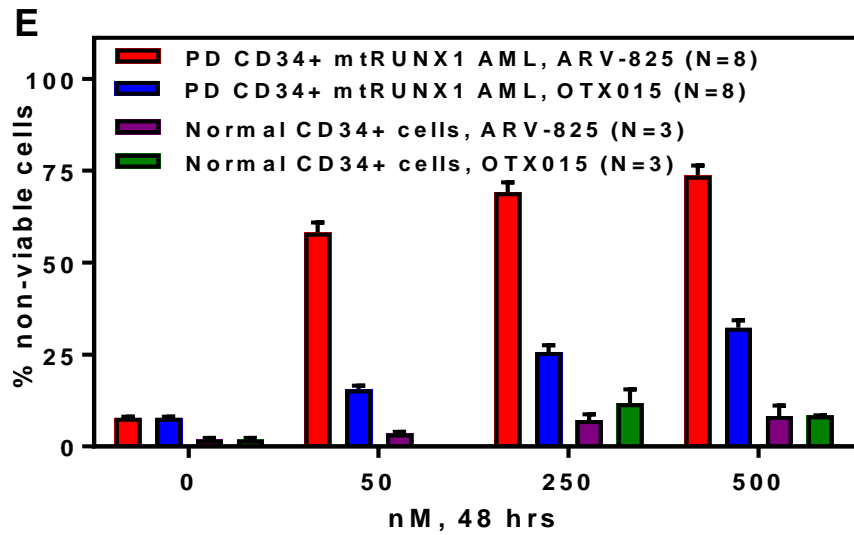
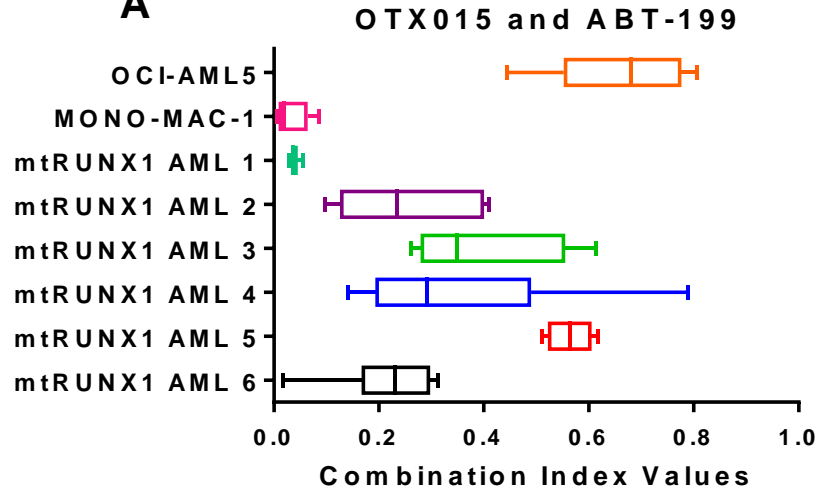
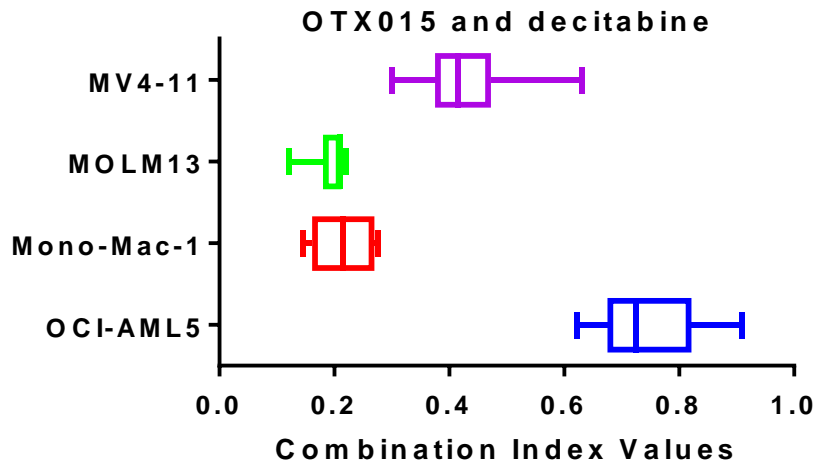
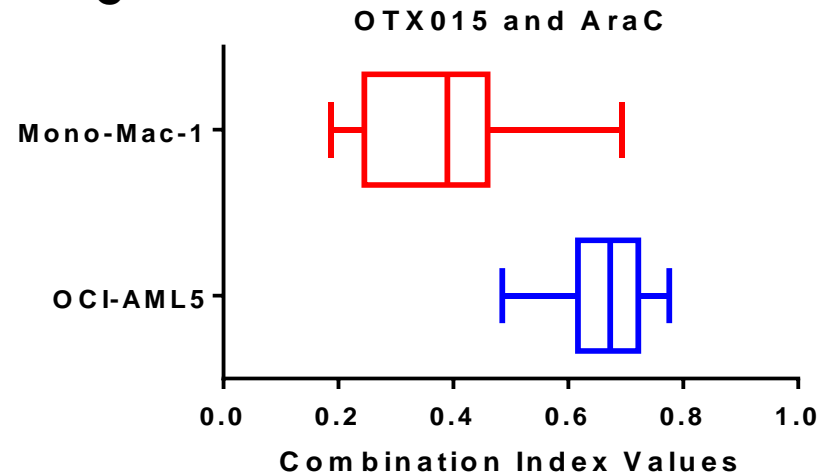


Figure S3





**A****B****C**

D

<u>MV4-11</u>			
OTX015 (nM)	DAC (nM)	Fa	CI Value
100	200	0.678	0.30050
150	300	0.711	0.41768
175	350	0.766	0.42370
190	380	0.816	0.39647
200	400	0.824	0.40641
250	500	0.752	0.62840

<u>MOLM13</u>			
OTX015 (nM)	DAC (nM)	Fa	CI Value
100	100	0.704	0.12135
300	300	0.799	0.21889
350	350	0.828	0.21228
375	375	0.843	0.20478
400	400	0.851	0.20586
500	500	0.876	0.20992

<u>Mono-Mac-1</u>			
OTX015 (nM)	DAC (nM)	Fa	CI Value
250	250	0.4884	0.24454
500	500	0.6062	0.21511
600	600	0.5969	0.27555
750	750	0.6315	0.26967
800	800	0.709	0.16123
900	900	0.7369	0.14468

<u>OCI-AML5</u>			
OTX015 (nM)	DAC (nM)	Fa	CI value
250.0	250.0	0.152	0.71532
250.0	500.0	0.149	0.73416
250.0	1000.0	0.175	0.62150
1000.0	250.0	0.401	0.90950
1000.0	500.0	0.440	0.79171
1000.0	1000.0	0.478	0.69338

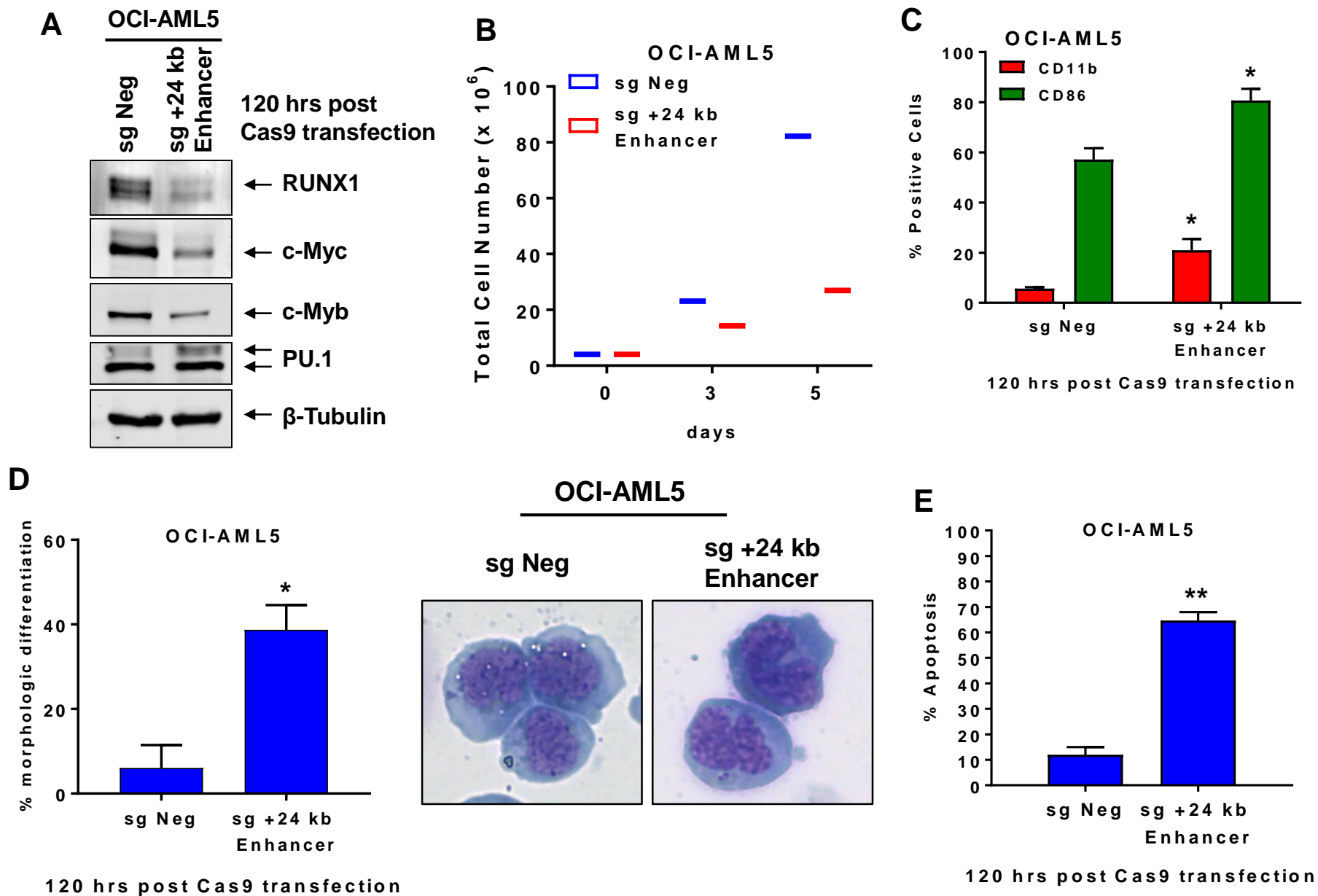
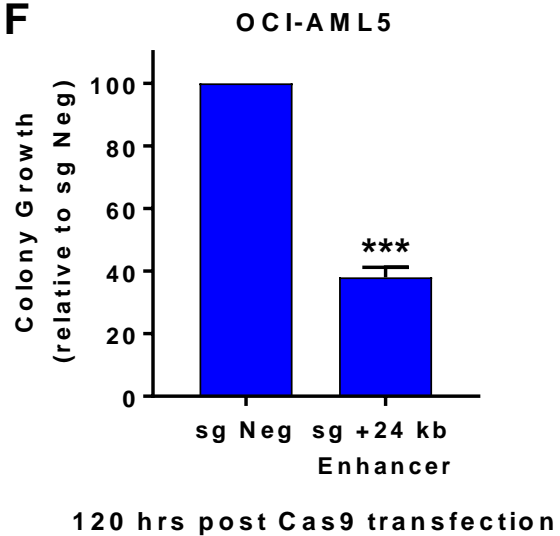
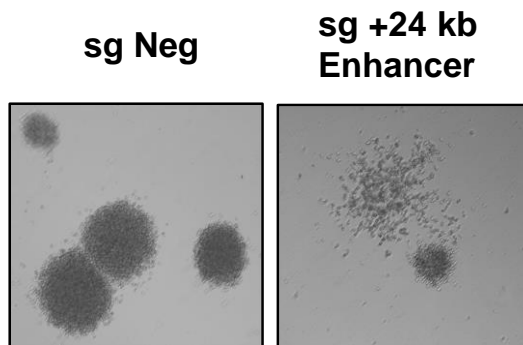


Figure S6

**F**

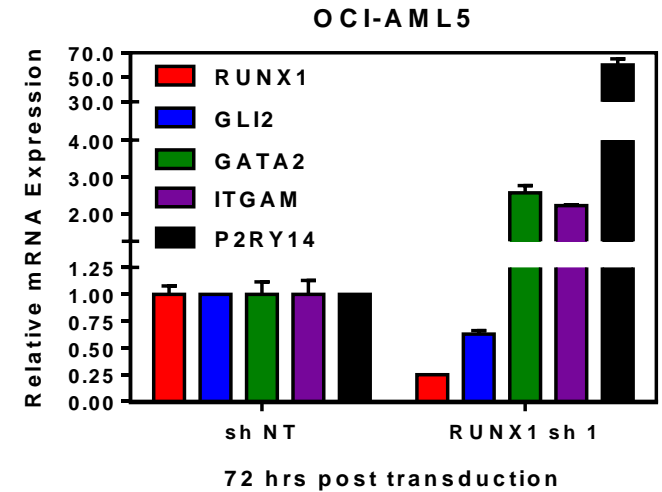
**OCI-AML5**

**Figure S6**

A

50 most upregulated genes	Log2 fold change over sh NT	50 most downregulated genes	Log2 fold change over sh NT
HIST2H2AB	3.45	SLC12A5	-1.78
RP1-34B20.21	3.31	RP11-38C17.1	-1.73
HIST1H2BI	3.24	HSH2D	-1.73
HIST1H4H	3.2	LTK	-1.68
HIST1H2BM	3.12	IL2RA	-1.53
HIST1H1B	2.99	HAL	-1.47
HIST1H2AE	2.93	FUT7	-1.45
HIST1H4A	2.91	MPO	-1.44
HIST1H4C	2.91	CTSG	-1.4
HIST1H3C	2.9	UGT3A2	-1.4
HIST1H2BE	2.9	CMAS	-1.38
HIST1H1D	2.88	LYPLA1	-1.36
HIST1H2AL	2.87	STARD3NL	-1.35
HIST1H3J	2.85	VIM	-1.34
HIST2H2BF	2.82	PRTN3	-1.32
HIST1H2BF	2.79	RTN4R	-1.32
HIST1H2AB	2.78	TTC27	-1.25
HIST1H1E	2.77	B3GNT7	-1.25
HIST1H4B	2.77	MOCS2	-1.24
HIST1H2BG	2.74	OSTC	-1.24
HIST1H2BB	2.73	DNAJC5B	-1.24
HIST1H2BL	2.71	SULT1A4	-1.23
HIST2H3D	2.68	EIF2S2	-1.23
HIST1H2BD	2.64	ANG	-1.22
HIST1H2AK	2.62	BZRAP1	-1.21
HIST1H4E	2.54	CXorf56	-1.19
P2RY14	2.41	SMIM24	-1.19
HIST2H2BE	2.4	MS4A3	-1.17
HIST1H4D	2.36	CD8A	-1.16
HIST1H2BN	2.18	ANXA3	-1.14
HIST1H2BH	2.13	MREG	-1.14
HIST1H2BJ	2.1	IRX3	-1.14
HIST2H3A	2.08	RHOU	-1.14
HIST2H3C	2.08	IL7R	-1.13
HIST1H2AM	2.02	AIG1	-1.13
HIST2H4B	2.02	SH3RF1	-1.13
C1orf186	1.94	THBS4	-1.1
TFPI	1.9	TRIM6	-1.1
HIST2H4A	1.87	PPP1R27	-1.09
HIST4H4	1.86	MPZL1	-1.09
HIST3H2BB	1.7	FAM46C	-1.06
ADORA3	1.68	PLGRKT	-1.06
ITGA9	1.62	KLHL15	-1.04
PCED1B	1.59	ATP5C1	-1.03
CTTN	1.55	GOLGA80	-1.03
SLC15A3	1.54	GOLGA8R	-1.03
P2RY13	1.5	UBXN2A	-1.02
ARHGAP6	1.49	CTC-534A2.2	-1.02
DMWD	1.47	STK26	-1.01

B



# Overlap of gene expression signature between ARV825, OTX015 and RUNX1 shRNA

A

mRNA target	RUNX1 shRNA	ARV-825	OTX015
RP1-34B20.21	3.31	4.03	4.86
HIST1H3C	2.9	2.11	1.9
HIST1H1D	2.88	2.39	2.11
HIST2H2BF	2.82	2.08	2.59
HIST1H2BF	2.79	2.83	2.62
HIST1H2BG	2.74	3.89	4.01
HIST2H3D	2.68	3.3	2.99
HIST1H2BD	2.64	3.49	3.4
HIST1H2AK	2.62	4.48	3.39
HIST2H2BE	2.4	2.49	3.39
HIST1H4D	2.36	4.86	3.91
HIST1H2BN	2.18	2.2	2.11
HIST1H2BH	2.13	5.09	2.88
HIST1H2BJ	2.1	3.38	4.24
HIST2H3C	2.08	5.08	3.95
HIST2H3A	2.08	5.07	3.95
HIST2H4B	2.02	4.47	4.7
HIST2H4A	1.87	4.45	4.76
HIST4H4	1.86	2.02	2.24
HIST3H2BB	1.7	4.06	2.7
HIST1H4J	1.41	2.16	1.43
HIST1H4K	1.3	2.23	1.39
HIST1H3H	1.09	4.25	4.26
HIST2H2AA3	1.07	2.85	4
HIST2H2AA4	1.06	2.85	3.98
HIST1H2BK	1.06	2.52	2.84
HIST1H2AG	1.05	3.74	3.19
ARRDC3	1.02	1.85	2.5
HELZ2	0.95	1.08	1.49
HIST2H2AC	0.82	2.24	2.41
SESN3	0.81	1.92	2.02
RGS2	0.77	1.38	2.18
MT1E	0.73	1.82	1.65
SPDYE1	0.73	1.75	1.1
NFAT5	0.73	1.71	1.59
HIST1H2AC	0.72	4.98	5.59
MT2A	0.71	2.37	2.43
FILIP1L	0.68	1.95	1.72
SYTL2	0.66	2.06	1.72
ZBED6	0.63	1.29	1.43
BTG2	0.61	1.68	1.64

B

mRNA target	RUNX1 shRNA	ARV-825	OTX015
HSH2D	-1.73	-3.69	-3.86
IL2RA	-1.53	-2.39	-2.42
FUT7	-1.45	-2.88	-2.48
TTC27	-1.25	-1.45	-1.46
B3GNT7	-1.25	-6.03	-4.48
GPR183	-1.15	-4.14	-3.12
RHOA	-1.14	-1.99	-1.56
IRX3	-1.14	-2.43	-1.5
IL7R	-1.13	-2.35	-2.27
TRIM6	-1.1	-2.15	-2.34
S1PR3	-0.97	-1.29	-1.33
ST3GAL4	-0.88	-1.34	-1.13
GLI2	-0.85	-3.14	-2.23
CXCL8	-0.83	-2.72	-1.21
CLEC5A	-0.81	-1.82	-3.13
ITPKA	-0.8	-2.4	-1.04
COL9A3	-0.78	-3.22	-1.54
RNASE10	-0.77	-2.36	-3.19
NOG	-0.76	-4.43	-1.86
NFE2	-0.74	-3.34	-1.58
RAB42	-0.73	-1.21	-1.89
TLR2	-0.71	-2.96	-1.29
KIF17	-0.68	-2.52	-2.94
RFX8	-0.63	-1.41	-2.33
THBD	-0.63	-2.26	-1.4
CBARP	-0.62	-2.27	-1.5
GYPE	-0.62	-3.94	-1.57
P2RY2	-0.61	-2.82	-2.36
CSRP3	-0.59	-2.02	-2.66
CXorf21	-0.59	-3.84	-3.15

Table S2

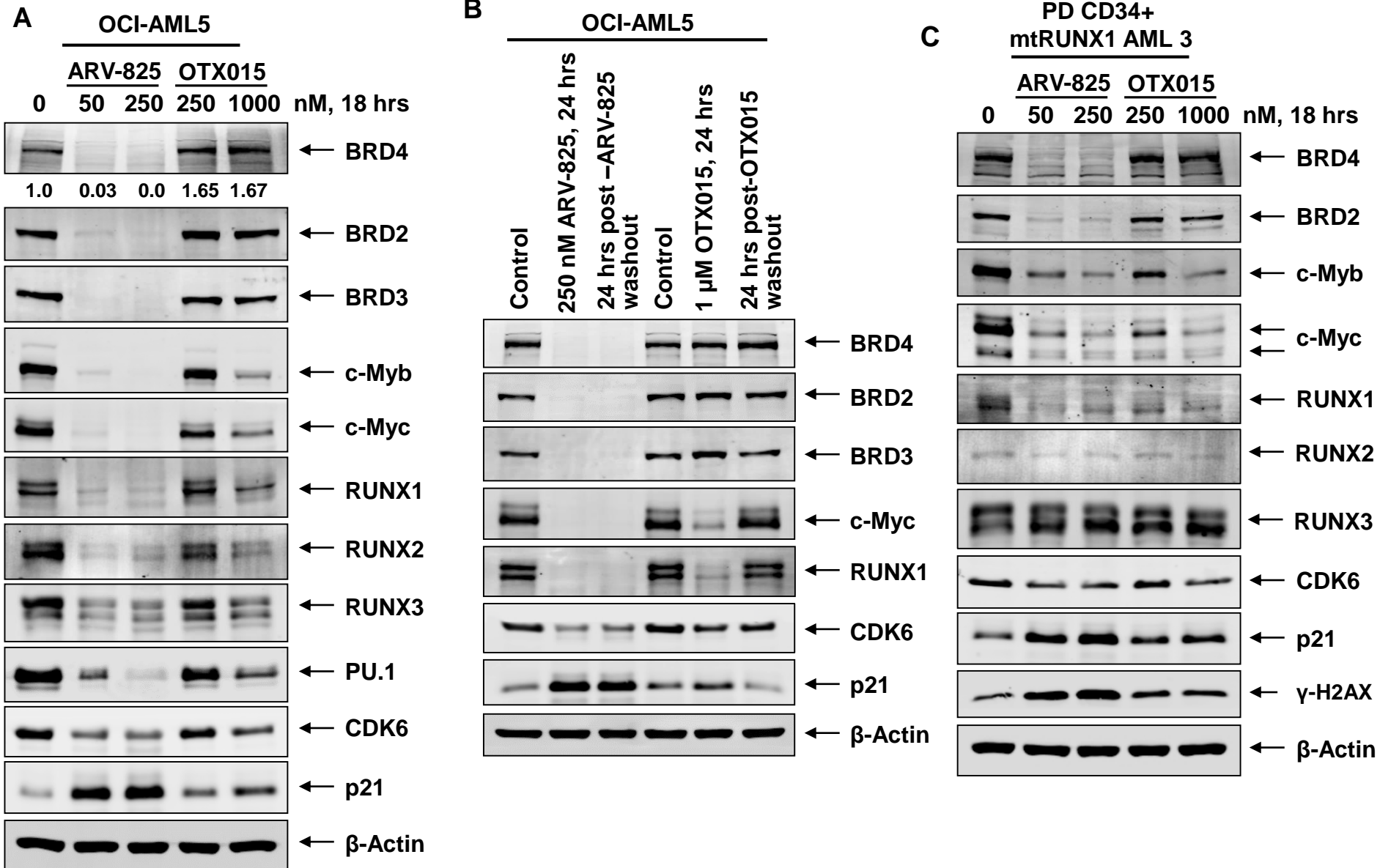
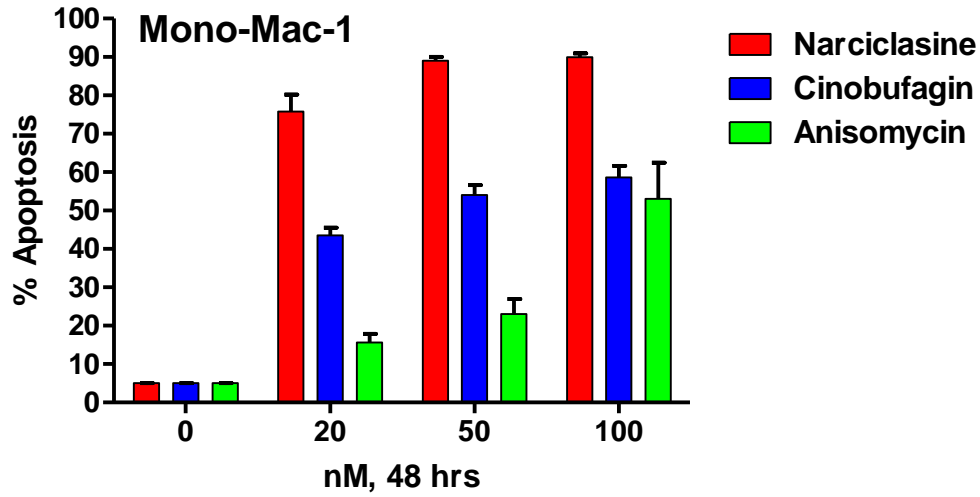


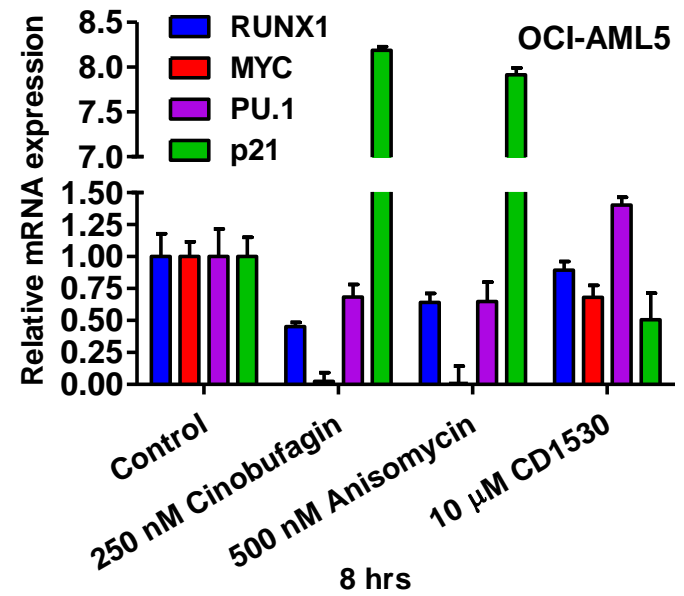
Table S3

Name of agent in Broad database	Expression Mimicker	Rank	Type of inhibitor
BRD-K03067624	emetine	1	anti-protozoa
BRD-K76674262	homoharringtonine	2	natural plant alkaloid
BRD-K36055864	cycloheximide	3	protein synthesis inhibitor
BRD-K80348542	cephaeline	4	an emetic and expectorant
BRD-K06792661	narciclasine	5	natural plant alkaloid
BRD-A26002865	verrucarin-a	6	protein synthesis inhibitor
BRD-K91370081	anisomycin	7	antibiotic; eukaryotic protein synthesis inhibitor
BRD-K08316444	rotenone	8	Pesticide; Complex I inhibitor
BRD-K32828673	chelidonine	9	acetylcholinesterase
BRD-K25737009	CD-1530	10	RAR $\gamma$ agonist; activates RAR alpha
BRD-A98444709	BRD-A98444709	11	6-(3,5-Dimethyl-1,2-oxazol-4-yl)-N-[(1-methyl-2-piperidinyl)methyl]-4-quinazolinamine
BRD-A71459254	cymarin	12	cardiac glycoside and an anti-arrhythmia
BRD-A93236127	digitoxin	13	cardiac glycoside. Phytosteroid
BRD-A68930007	ouabain	14	Na <sup>+</sup> /K <sup>+</sup> -ATPase pump inhibitor
BRD-U33728988	QL-X-138	15	BTK/MNK dual kinase inhibitor
BRD-K97365803	PI-828	16	PI3K inhibitor
BRD-U68942961	JW-7-24-1	17	LCK inhibitor
BRD-K12502280	TG-101348	18	JAK2 inhibitor (also inhibits BRD4)
BRD-K18518344	digitoxigenin	19	Cardenolide
BRD-A85860691	chaetocin	20	HMT SU(VAR)3-9 inhibitor
BRD-U86922168	QL-XII-47	21	inhibits dengue virus
BRD-K88622704	BRD-K88622704	22	6-(3,5-Dimethyl-1,2-oxazol-4-yl)-N-(2-ethoxybenzyl)-4-quinazolinamine
BRD-K06750613	GSK-1059615	23	dual inhibitor of PI3K $\alpha/\beta/\delta/\gamma$ and mTOR
BRD-K10361096	BRD-K10361096	24	N-[4-({[6-(3,5-Dimethyl-1,2-oxazol-4-yl)-4-quinazoliny]amino)methyl}phenyl]acetamide
BRD-K22385716	LY-303511 (inhibits BRD2,3,4)	25	PI 3-kinase inhibitory
BRD-K63606607	bufalin	26	cardiotonic steroid
BRD-K52163391	BRD-K52163391	27	6-(3,5-Dimethyl-1,2-oxazol-4-yl)-N-[(3-methyl-2-thienyl)methyl]-4-quinazolinamine
BRD-K13646352	Midostaurin	28	FLT3 kinase inhibitor; multi-kinase inhibitor
BRD-A94756469	digoxin	29	cardiac glycoside
BRD-K51318897	fenbendazole	30	benzimidazole anthelmintic
BRD-K02407574	Parbendazole	31	benzimidazole anthelmintic
BRD-A45333398	periplocymarin	32	Natural cardiac glycoside
BRD-K71265179	BRD-K71265179	33	9-(4-Methylbenzoyl)-9H-carbazole
BRD-K54256913	MK-1775	34	Wee-1 kinase inhibitor
BRD-K60623809	SU-11652	35	ATP-competitive tyrosine kinase inhibitor
BRD-K61323504	SB-225002	36	potent, and selective CXCR2 antagonist
BRD-A80502530	cinobufagin	37	bufanolide steroid
BRD-K67506692	tyrphostin-AG-126	38	protein tyrosine kinase inhibitor
BRD-K30707190	PNU-74654	39	$\beta$ -catenin /T cell factor 4 (Tcf4) inhibitor
BRD-K84595254	strophanthidin	40	cardiac glycoside; activity similar to ouabain
BRD-K00337317	NU-7441	41	potent and selective DNA-PK inhibitor
BRD-K35716340	BRD-K35716340	42	9-[2-(1H-Benzimidazol-2-yl)ethyl]-9H-carbazole
BRD-K67075780	TGX-115	43	inhibitor of PI 3-K isoforms p110 $\beta$ /p110 $\delta$
BRD-A62182663	YK-4279	44	inhibitor of RNA Helicase A
BRD-K94441233	mevastatin	45	HMG-CoA reductase inhibitor; Statin

A



B



C

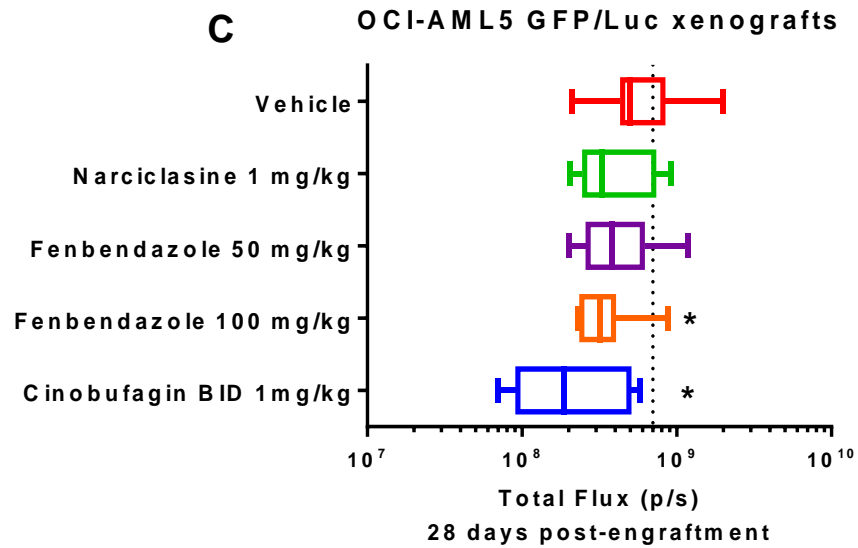
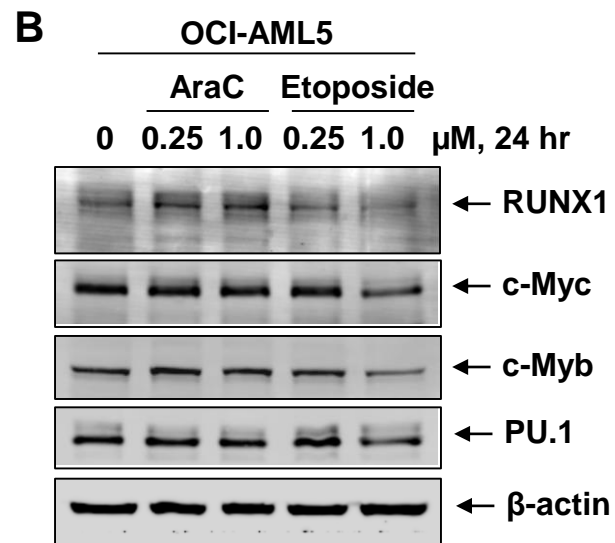
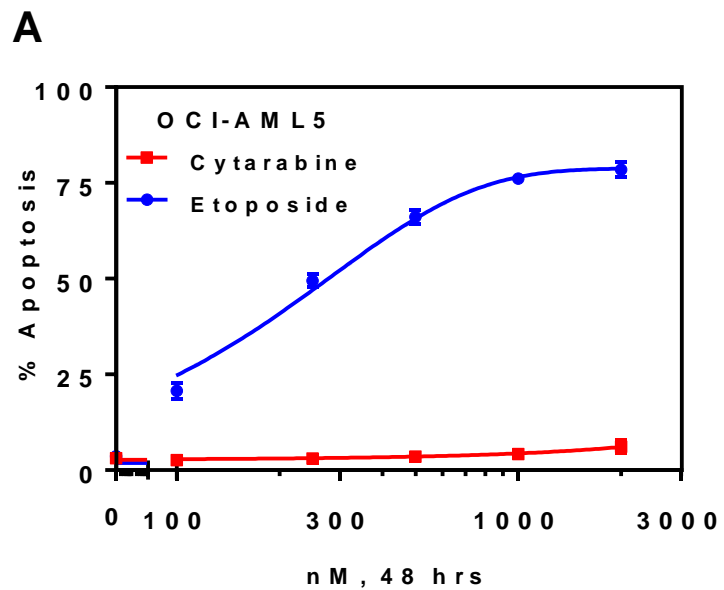


Figure S10



**Supplemental Table 4. Oligonucleotide primers utilized in these studies**

<b>Primer Name</b>	<b>Sequence 5'-3'</b>
RUNX1 sh 1 For	CCGGGAACCAGGTTGCAAGATTTAACTCGAGTTAAATCTTGCAACCTGGTTCTTTTT G
RUNX1 sh 1 Rev	AATTCAAAAAGAACCAGGTTGCAAGATTTAACTCGAGTTAAATCTTGCAACCTGGTTC
RUNX1 sh2 For	CCGGGAACCACTCCACTGCCTTTAACTCGAGTTAAAGGCAGTGGAGTGGTTCTTTTT G
RUNX1 sh2 Rev	AATTCAAAAAGAACCACTCCACTGCCTTTAACTCGAGTTAAAGGCAGTGGAGTGGTT C
P2 Promoter BgIII.for	GA AGA TCT CCT GAC TAG GAA ACT CTT CGC TGG C
P2 Promoter HindIII.rev	GCA AAG CTT GCA GAG GTT GAC TTC CTT CTG GC
+24 kb Enhancer Sall.for	GCA GTC GAC GGC ATT ACA GGC CTC ATG AGG ATG TAG
+24 kb Enhancer AfeI.rev	GCA AGC GCT CAC TTC TCT GGG AAG CCT CTT GAC AC
RUNX1 prom 1 For	AAAACATCCAGCCAAGAAGC
RUNX1 Prom Rev	CAACCTCTGCTGCTTCTCCT
RUNX1 Enhancer For	ATAACTGCCGAAGTGCCTTG
RUNX1 Enhancer Rev	TGCTATTCCACAGAAGGATGG
RUNX1 P1 Prom 1 For	CCTGTGGTTTGCATTCAAGT
RUNX1 P1 Prom 1 Rev	TTTGGGCCTCATAACAACC
RUNX1 P1 Prom 2 For	GCTTCCTCCTGAAAATGCAC
RUNX1 P1 Prom 2 Rev	GTAGGGCTAGAGGGGTGAGG
RUNX1 +24 kb Enhancer 1 For	ACAGGATGCCTCCATCTGAG
RUNX1 +24 kb Enhancer 1 Rev	TCTGGGAAGCCTCTTGACAC
RUNX1 +24 kb Enhancer 2 For	CCTGTGGTTTTCTCGCTCTC
RUNX1 +24 kb Enhancer 2 Rev	CTTTCAAAGAGCCTGGGATG